



TECHNISCHE
UNIVERSITÄT
WIEN

DIPLOMARBEIT

Gold Nanocluster als homogene und heterogene Katalysatoren für selektive Hydrierung

ausgeführt am

Institut für Materialchemie
der Technischen Universität Wien

unter der Anleitung von

Privatdoz.in Dr.in Noelia Barrabés Rabanal

durch

Rareş Banu
Getreidemarkt 9, 1060 Wien

Wien, 10/07/2024



TECHNISCHE
UNIVERSITÄT
WIEN

MASTER THESIS

Gold Nanoclusters as Homogeneous and Heterogeneous Catalysts for Selective Hydrogenation

carried out at the

Institute of Materials Chemistry
of TU Wien

under the supervision of

Privatdoz.in Dr.in Noelia Barrabés Rabanal

by

Rareş Banu
Getreidemarkt 9, 1060 Vienna

Vienna, 10/07/2024

EIDESSTÄTTLICHE ERKLÄRUNG: Ich erkläre hiermit an Eides statt, dass ich die vorliegende Arbeit selbstständig verfasst, andere als die angegebenen Quellen/Hilfsmittel nicht benutzt, und die den benutzten Quellen wörtlich und inhaltlich entnommenen Stellen als solche kenntlich gemacht habe.

STATUTORY DECLARATION: I hereby declare that I have authored this thesis independently, that I have not used other than the declared sources/resources, and that I have explicitly marked all material which has been quoted either literally or by content from the used sources.

Kurzfassung

Hydrierungsreaktionen sind ein wichtiger Bestandteil einer Vielzahl von Industrien in der heutigen Welt, von der Öl- und Gasindustrie bis hin zu großen Pharmakonzernen. Aus diesem Grund wurde viel Forschung in die Entwicklung hocheffizienter Katalysatoren gesteckt, wobei traditionell Metalle der Platingruppe verwendet werden. Obwohl mit den Katalysatoren, die hohe Umwandlungs- und Selektivitätsraten aufweisen, hervorragende Ergebnisse erzielt wurden, bleiben bestimmte Probleme bestehen. Um hohe Selektivitätsniveaus zu erreichen, müssen die Katalysatoren häufig modifiziert oder vergiftet werden, was die Katalyse weniger effizient macht. Darüber hinaus fehlt ein wirkliches Verständnis des katalytischen Prozesses auf atomarer Ebene. Aus diesem Grund ist es notwendig, neue Möglichkeiten zu erkunden.

Ligandengeschützte Goldnanocluster sind eine relativ neue Klasse atomar präziser Materialien, deren Eigenschaften in hohem Maße einstellbar sind. Es hat sich gezeigt, dass die Wahl der Liganden, wie Thiolate oder Phosphine, die Struktur, Stabilität und Anwendbarkeit von Goldnanoclustern maßgeblich beeinflusst. Eine vielversprechende Anwendung für diese Metallnanocluster ist die Katalyse, sowohl in homogenen als auch heterogenen Systemen, wo sie ideale, wohldefinierte aktive Zentren zur Aufklärung der Struktur-Reaktivitäts-Beziehung bereitstellen.

In dieser Arbeit wurden Goldnanocluster bei der heterogenen Semihydrierung von Alkinen und der homogenen Reduktion von Ketonen zu Alkoholen getestet. Untersucht wurden die Auswirkungen von Ligandentypen, Ligandenpopulationen um den Metallkern, ihre Wechselwirkungen mit Trägern sowie die Auswirkung der Vorbehandlung. Es wurden starke Ligand-Träger-Wechselwirkungen beobachtet, einschließlich der Migration der Liganden zu Oxidoberflächen, wodurch neue aktive Zentren entstanden, sowie ein deutlicher Einfluss der Vorbehandlung. Im homogenen System wurde der Effekt der Metall-Ligand-Grenzfläche durch ihren Einfluss auf die katalytische Aktivität sichtbar. Die Ergebnisse zeigen, wie wichtig es ist, den Katalysator auf atomarer Ebene zu verstehen und alle strukturellen Aspekte beim Entwurf und der Optimierung eines katalytischen Systems zu berücksichtigen, wodurch Goldnanocluster ideale Kandidaten für solche Anwendungen sind.

Abstract

Hydrogenation reactions are an important part of a multitude of industries in today's world, ranging from oil and gas to big pharma. Due to this, a lot of research has gone into designing highly efficient catalysts, with platinum group metals being traditionally used. While great results have been achieved, with the catalysts showing high conversion and selectivity rates, certain problems remain. In order to reach high selectivity levels, the catalysts must often be modified or poisoned, making the catalysis less efficient. Furthermore, a true understanding of the catalytic process at an atomic level is missing. Because of this, it is necessary to explore new possibilities.

Ligand protected gold nanoclusters are a relatively novel class of atomically precise materials, which properties are highly tuneable. It has been shown that the choice of ligands, such as thiolates or phosphines, significantly influences the structure, stability and applicability of gold nanoclusters. One promising application for these metal nanoclusters is catalysis, both in homogeneous and heterogeneous systems, where they provide ideal, well-defined active sites to elucidate the structure-reactivity relationship.

In this thesis, gold nanoclusters were tested in the heterogeneous semihydrogenation of alkynes and the homogeneous reduction of ketones to alcohols. The effects of ligand types, ligand populations around the metal core, their interactions with supports, as well as the effect of pretreatment were investigated. Strong ligand-support interactions were observed, including ligand migration to oxide surfaces, creating new active sites, as well as a clear influence of pretreatment. In the homogeneous system, the effect of metal ligand interface became visible, through its impact on the catalytic activity. The results show the importance of understanding the catalyst at an atomic level and considering all structural aspects when designing and optimizing a catalytic system, placing gold nanoclusters as ideal candidates for such applications.

Acknowledgments

The practical work of this thesis was done at the Institute of Materials Chemistry of the TU Wien. First of all, I would like to thank Privatdoz.in Dr.in Noelia Barrabés for giving me the opportunity to conduct my Master Thesis in her group, ClusCat. Your guidance and trust, starting with my Bachelor Thesis, helped shape me as a scientist and person.

Next, I would like to thank all members of the group, Lisa Lenz and Sebastian Mößlacher, for bearing with me in the lab and the office, for making me laugh and keeping me motivated. I would also like to extend my thanks to other members of the institute and visiting students, for all your helpful discussions, especially to Alberto Tampieri. Moreover, I want to mention the people whom I had the pleasure to share several synchrotron beam times with, Adea Loxha (for all the night shifts painfully studying for exams, worrying about weird noises and playing cards), Nicole Müller, Stylianos Spyroglou and Pietro Mariani.

Lastly, I want to thank my family and friends, especially my girlfriend Magdalena Weinstabl for supporting me during late nights working, my best friend Jonathan Swanson for reminding me of the light at the end of the tunnel and my parents and sister for always believing in me and being by my side.

Contents

Contents	iv
1. Introduction	1
1.1. Monolayer Protected Gold Nanoclusters	2
1.1.1. Synthesis	2
1.1.2. Structure	3
1.2. Semihydrogenation of Alkynes	5
1.2.1. Previous Works	6
1.2.2. Gold in Heterogeneous Catalysis	7
1.3. Reduction of Ketones to Alcohols	9
1.3.1. Current Works	9
1.3.2. Gold nanoclusters in Ketone Reduction	10
2. Motivation of the Thesis	11
3. Experimental Section	12
3.1. Experimental	12
3.1.1. Materials	12
3.1.2. Nanocluster Synthesis	12
3.1.3. Preparation of supports	16
3.1.4. Preparation of supported nanoclusters	16
3.1.5. Catalytic tests	16
3.1.6. X-Ray Absorption Fine Structure (XAFS) Spectroscopy	17
3.1.7. Characterization	18
4. Results and Discussion	20
4.1. Heterogeneous Semihydrogenation of Alkynes	20
4.1.1. Catalytic Activity	21
4.1.2. Support Characterization	25
4.1.3. XAFS Analysis	25
4.2. Homogeneous Hydrogenation of Ketones	34
4.2.1. Catalytic Activity in Homogeneous Phase	35
5. Conclusions and Outlook	38

A. Appendix	42
List of Figures	47
List of Tables	49
Bibliography	50

Abbreviations

2-MBT	(<i>S</i>)-2-methyl-1-butanethiol
2-PET	2-phenylethanethiol
DCM	methylene chloride
DFT	Density Functional Theory
EtOAc	Ethylacetate
EtOH	Ethanol
EXAFS	Extended X-Ray Absorption Fine Structure Spectroscopy
GC	Gas Chromatography
GSH	<i>L</i> -glutathione
HPLC	High Performance Liquid Chromatography
iPrOH	2-propanol
MALDI	Matrix-Assisted-Laser-Desorption-Ionization
MeOH	methanol
MS	Mass Spectrometry
NMR	Nuclear Magnetic Resonance
PPh₃	triphenylphosphine
SEC	Size Exclusion Chromatography
THF	tetrahydrofurane
UV-Vis	Ultraviolet-Visible
XAFS	X-Ray Absorption Fluorescence Spectroscopy
XANES	x-Ray Absorption Near Edge Structure Spectroscopy
XRD	X-Ray Powder Diffraction

1. Introduction

Hydrogenation reactions are of great importance to many industries in today's society, including the oil and gas and pharmaceutical industries.^[1, 2] Two reactions that drew lots of attention in the past years are the semihydrogenation of alkynes and the reduction of ketones to alcohols.^[3-8]

Alkynes hold immense synthetic potential. However, in certain contexts, converting alkynes to alkenes becomes crucial, as these are versatile building blocks for natural products, pharmaceuticals, and fine chemicals.^[9-11] However, limiting the reaction to hydrogenation to the alkene is a challenge that requires careful catalyst design. Widely used are palladium based catalysts^[10, 12, 13], which can however lead to undesired side reactions, such as complete hydrogenation to ethane or oligomerization resulting in the deposition of C₄+ liquid oil on the catalyst surface. Further optimization of catalysts is therefore necessary to address these challenges.

Reducing ketones to alcohols is a process of importance especially in the pharmaceutical industry.^[6, 7] Traditionally, stoichiometric reducing agents such as LiAlH₄ or Na(BH)₄ are used. While they generally show a good yield, they are not selective and the stoichiometric amount needed makes them impractical. Recently, several approaches have been explored, including the use of enzymes^[6] or organic catalysts^[7, 8]. While these types of catalysts show better selectivity and in some cases even enantioselectivity, they are often highly specific and in need of tedious modifications, in order to make them viable for a wider range of substrates^[8].

Considering the problems faced across these fields, it appears necessary to explore new approaches. Inorganic (nano)catalysts offer not only good activity and selectivity, but are also simple to synthesize and are not substrate specific.^[4, 5] Because of this, transition metal and especially noble metal catalysts have become very popular. Of those, an up-and coming player gold-based catalysts^[14, 15]. They have been found to be active in a multitude of hydrogenation reactions, showing good selectivity and tuneability. Interestingly, reports have shown that when going away from bulk gold, the size-effect on the catalysis is very pronounced.^[14] In this field, one interesting and novel class of materials is that of gold nanoclusters. Recent studies have shown their prowess as catalysts for hydrogenation reactions, setting them as promising, improved alternatives to the current options.^[14] This work delved into the different ways nanoclusters can be used as catalysts in both homogeneous and heterogeneous systems, for the semihydrogenation of alkynes and the reduction of ketones to alcohols, unveiling critical structure-activity correlations, that can be used in order to tune the catalyst for maximum efficiency.

1.1. Monolayer Protected Gold Nanoclusters

As previously mentioned, a great challenge in catalysis is that of understanding the structure and evolution of the catalyst exactly, thereby being able to gauge the influence of the different factors on the success of the reaction. Gold nanoclusters present as an interesting new class of materials, with properties between those of molecules and bulk. As size decreases, the possibility for plasmon resonance disappears and a band gap comes to life. Furthermore, the fcc symmetry of bulk gold is broken and size-dependent structures appear. Under a critical size, the properties of the material stop to scale with size and become utterly dependent on the number of atoms in the nanocluster. At this point, only certain particle sizes remain stable, so-called "magic-number" clusters. These are based on the super-atom model and follow similar principles like regular molecular complexes, where the most stable structures are those with a full electron shell.^[16, 17] Because of their atomic precision, gold nanoclusters are the ideal bridge between model systems and industrial catalysts, allowing researchers to conduct experiments using a system that is atomically defined and therefore highly tuneable, similar to model catalysts, but that works under ambient conditions, similar to industrial catalysts.

1.1.1. Synthesis

The standard protocol for the synthesis of ligand protected Au nanoclusters is defined by a couple of optimized conditions: starting from a Au(III) salt, a generous excess of ligand is added to the gold in order to reduce it to the Au(I)-SR polymer. Subsequently, a reducing agent such as NaBH₄ is added in excess, to further reduce to gold to Au(0).^[16] This method leads to a polydisperse product with a narrow size-distribution, which can then be further purified by HPLC^[18] or polyacrylamide gel electrophoresis (PAGE).^[19] The major problem, however, are the typically rather low yields of the synthesis,^[16] making the further investigation of the product troublesome. Nevertheless, there has been a lot of progress since the beginning of metal nanocluster chemistry, with two different methods as the established standards: the size-focusing synthesis, and the ligand exchange-induced size/structure transformation (LEIST), which allowed for the systematic synthesis of atomically precise Au nanoclusters in relatively high yield, but which will not be dealt with further in this thesis.^[16]

Size-Focusing Synthesis

The first report of a kinetically controlled synthesis of monodisperse Au nanoclusters was presented by Zhu *et al.*^[20] in 2008 for the synthesis of the Au₂₅(SR)₁₈ nanoclusters. They rationalized that, if one could control the kinetics of the synthesis, the chemical conditions could be adapted, so that a monodisperse product is created, while clusters of other sizes are repressed.^[20] While the general steps of the synthesis remained the same, it was found that by controlling the kinetics of the formation of the Au(I)-polymer through temperature control and by optimizing the stirring speed, a higher yield could be obtained.^[20] An example of this

synthesis is shown in Figure 1.1.

In the case of phosphine protected gold nanoclusters, the synthesis protocol remains mainly similar. The greatest difference lays in the use of different counter-ions, which are always part of the final cluster structure.^[17] Furthermore, the use of different reducing agents, other than $\text{Na}(\text{BH})_4$, has been explored and shown to help steer the synthesis towards clusters of different sizes.^[17] The first phosphine cluster to be successfully synthesized was the Au_{11} nanocluster, which was discovered in 1969 and which structure was first elucidated by Simon *et al.* in 2013^[21]. In order to expand the range of clusters available, researchers broke away from the one phase synthesis and attempted a two phase protocol, which in some cases lead to the formation of more stable and robust nanoclusters.^[22]

The core idea of the size-focusing method is that by controlling the kinetics of the formation of the Au(I)-polymer, it is possible to, through a size-focusing etching process, synthesize clusters of different sizes in high purity and high yield.^[16] The size-focusing process bases on the idea that clusters of certain sizes, so-called magic number nanoclusters, are more stable than others, and thus survive the etching process, similar to the idea of "survival of the fittest".^[16]

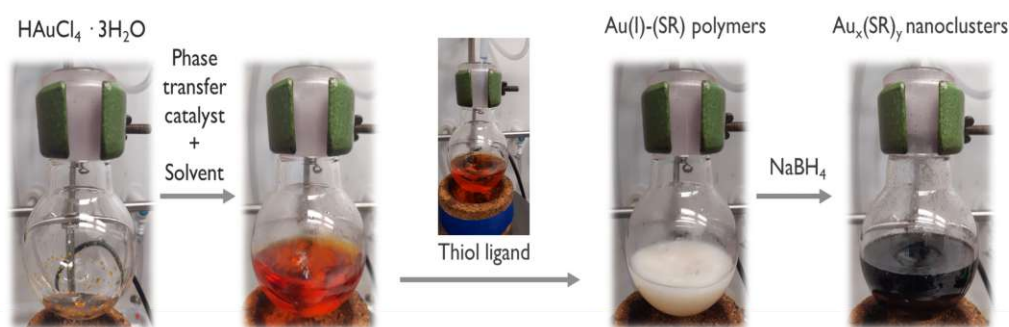


Figure 1.1.: Example of the size-focusing synthesis method for thiolate protected gold nanoclusters.

1.1.2. Structure

Early work on the structure determination of thiolate protected nanoclusters proposed a compact gold core, covered by an uniform Au/S interface.^[23] The first cluster of which the electronical structure was fully disclosed was $\text{Au}_{38}(\text{SR})_{24}$, where SR stands for thiolate.^[24]

The first proposed structure, calculated by density functional (DFT) calculations, consisted of a truncated-octahedral, face-centered-cubic Au_{38} core, which was protected by a monolayer of 24 SR units.^[24] This proposition was, however, soon challenged by Garzón and co-workers,^[25] who proposed a new, disordered structure, which presented at around 4 eV lower energy levels than the truncated-octahedral one. It is composed of an amorphous, 16 atom Au core, with the remaining 22 Au atoms arranged at irregular intervals, and the thiol ligands binding to the cluster surface.^[25]

In 2006, however, a new, revolutionary model was presented: the "Divide and Protect" model.^[26] The proposed structure consisted of six Au(SR)₄ units, surrounding a Au₁₄ core, allowing for a sterically improved arrangement of ligands on the core. Furthermore, the gold atoms in the core were found to have metallic character (i.e. Au⁰), and the ones in the Au(SR)₄ units to be oxidised (i.e. Au⁺).^[27]

This model has however been improved upon by Lopez-Acevedo and co-workers,^[28] who, building on the work of Jiang *et al.*^[2] proposed a bi-icosahedral Au₂₃ core, that is stabilised by three monomeric staple units (Au(SR)₂) arranged around the equatorial region, and three dimeric staples (Au₂(SR)₃) at each of the two long ends of the cluster.^[28] Furthermore, it was proposed that the long staples are arranged in a rotating manner, leading to chirality in the cluster.^[28]

The breakthrough method for the total-structure-determination of gold nanoclusters was, however, not theoretical, but experimental, with the help of single-crystal XRD measurements. This was first achieved by Jadzinsky *et al.*^[29] who managed to crystallize the Au₁₀₂(SR)₄₄ cluster, and measure its single-crystal XRD spectrum. This method has been built upon since then and many more cluster structures could be elucidated.

Apart from thiolate protected nanoclusters, another common type of ligands are the phosphines. Perhaps the most famous such cluster is the Au₁₁ nanocluster, which structure was first elucidated in 1969.^[16] Following this, several other clusters of similar sizes were discovered shortly after, by independent groups.^[16] In contrast to the Au-S bond, the Au-P is comparably weak, allowing more flexibility for the clusters and making them favourable for catalysis applications.^[17] Furthermore, they do not show the staple configuration seen in thiolate protected nanoclusters. In this case, the ligands are directly bound to the gold core, through dative covalent bonds.^[17] An example of the structure of a thiolate and a phosphine protected cluster is depicted in Figure 1.2.

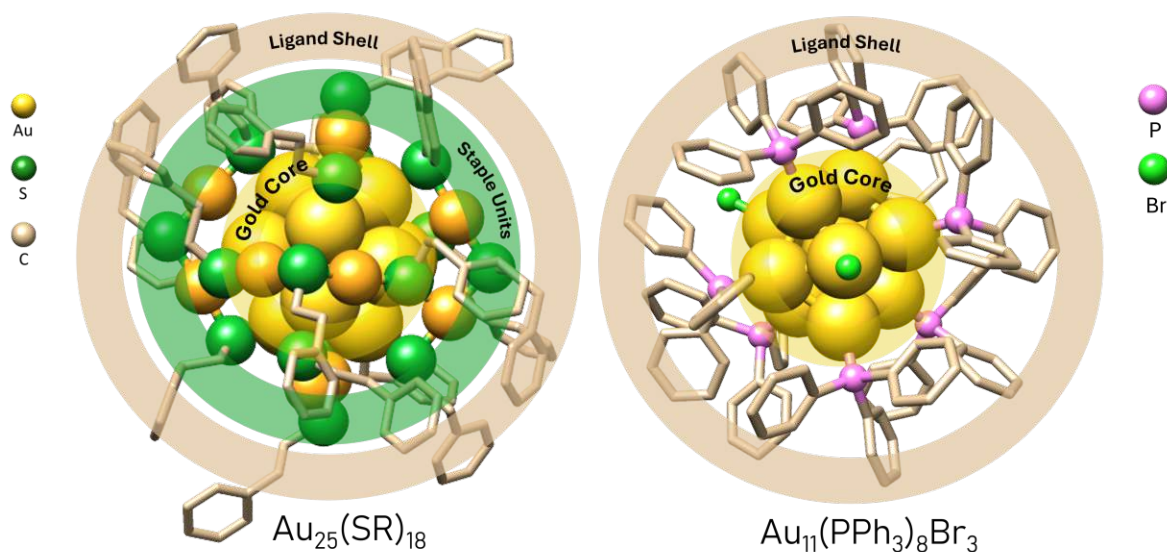


Figure 1.2.: Detailed structure of two prevalent nanoclusters, exemplifying the similarities and differences between thiolate and phosphine protected nanoclusters.

1.2. Semihydrogenation of Alkynes

The first part of this thesis focuses on the use of supported gold nanoclusters as heterogeneous catalysts in the semihydrogenation of phenylacetylene to styrene. The reaction is displayed in Figure 1.3 As previously mentioned the selective hydrogenation of alkynes to alkenes is a prevalent reaction, especially in the oil and gas industry, where alkynes are often found as impurities in the feed.^[1] This reaction is often referred to as the semihydrogenation of alkynes and follows the Horiuti-Polanyi mechanism. Hereby, the hydrogen adsorbs to the metal surface and dissociates, after which the alkyne adsorbs and the two formed hydrides bond to the unsaturated bond. Finally, the product desorbes.^[30] Typically, the adsorption barrier for alkynes on transition metals is lower than that of alkenes, meaning that they should be reduced first. However, as with most reactions in chemistry, there is a balance between the two processes, which is mostly depended on the relative concentration of the two compounds. Several approaches have been developed in order to control or monitor this reaction, ranging from spectroscopic monitoring of the reaction mixture to poisoning the catalysts.^[3]

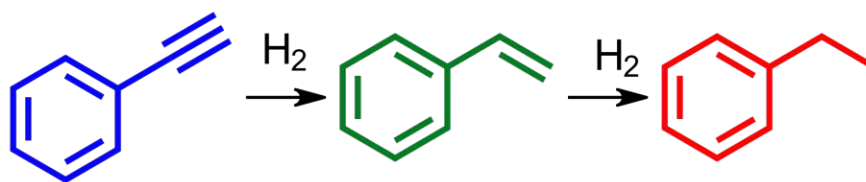


Figure 1.3.: Reaction pathway of the reduction of phenylacetylene (blue) to styrene (green; the desired product) and finally to ethylbenzene (red; undesired product).

1.2.1. Previous Works

Traditionally, Pd based catalysts are used for this process. While they are very active, the lack of selectivity due to the strong adsorption of the alkene to the Pd, owed to the strong π – bond, leading to overhydrogenation and polymerisation.^[5] A classic solution to gain control over the reaction is to poison the catalyst with Pb and quinoline, leading to the so-called Lindlar catalyst.^[3, 5] While this catalyst has several advantages, such as its heterogeneous nature, easy synthesis and improved selectivity, several issues remain, such as its toxicity due to Pb, lack of selectivity for some alkynes and its reproducibility.^[3] It is therefore necessary to search for alternatives.

Recently, the use of nanomaterials has become more and more popular. A recent study shows that the use of chemically modified PdIn Metal Organic Frameworks (MOFs), a more efficient semihydrogenation process can be achieved.^[5] Here, Martinez *et al.* explored a novel way to synthesize these type of MOFs, that uses a reductive chemical treatment, instead of direct pyrolysis. The advantage of this is the formation of PdIn bimetallic nanoparticles, which were then shown to regulate the activity of Pd in the semihydrogenation reaction, whereby the role of In is key.^[5] While this approach improves upon the selectivity and stability of conventional catalysts, the use of In to regulate activity is similar to the use of Pb, thereby leaving the problem of toxicity.

Another alternative presented by Albani and co-workers is the use of sulfides as ligands on Pd nanoparticles.^[12] They found that by supporting these structures, they could create highly stable catalysts with unique geometries and electronic structures. By incorporating sulphur into the Pd nanoparticles, atomically precise Pd_3S phases were formed, which allow for the selective hydrogenation of alkynes of multiple geometries. These catalysts were shown to have exceptionally high activity rates and stability, as compared to other state-of-the-art catalysts.^[12] This goes to show that the use of sulphur, as a chemically more abundant element than, for example, indium, it is possible to gain exceptional results, while also diminishing the issue of toxicity.

Apart from Pd, other metals have also been explored in a work by Bridier *et al.* such as Ni, Cu, Cu-Ni alloys and Au.^[10] By combining catalytic tests with DFT calculations, they were able to explain the different product distribution observed by each catalyst, allowing them to understand the systems better. It was found that by allowing metals, the conversion and se-

lectivity of catalyst can be vastly improved. They concluded that a ternary catalyst composed of Ni-Cu-Fe showed the best selectivity, with over 90 % and complete conversion. Furthermore, they were able to understand that changes in the structure of the catalysts caused a shift in the product distribution, hereby showing that considering the atomic structure of the catalyst is of great importance when designing a system.^[10]

1.2.2. Gold in Heterogeneous Catalysis

Considering the works done on such reactions using noble metal nanoparticles and keeping in mind the influence the catalyst structure has on the catalytic process, it is worth looking into another metal, often overlooked when talking about catalysis. Gold was long thought to be catalytically inactive, until it was discovered that when made on the nanoscale, it could catalyse the oxidation of CO at extremely low temperatures^[31]. Starting from then, many works have been done using Au as catalyst in many reactions, some of which being selective hydrogenations^[14, 32–34]. One of the most interesting findings of gold catalysis is the dependency on the particle size, a fact which already gives a hint to the importance of the structure of catalysts.^[14]

Nikolaev and Smirnov investigated the efficiency of gold nanoparticles in the heterogeneous semihydrogenation of phenylacetylene.^[35] The study found that these structures supported on Al₂O₃ show remarkable activity, selectivity and stability in this reaction. Furthermore, they concluded that a smaller particle size improved the catalysis, explaining this phenomenon through the increase in surface and corner sites, as well as the decrease in electron density around the surface of the particles, due to the alumina support.^[35] This account further underlines the importance of the structure of the catalyst, especially in regard to the particle size, as well as the effect of the support not only on the reaction, but on the catalyst itself, showing that the two interact with each other.

Continuing, a recent review^[15] shows the importance of gold in catalysis. They underline four key factors that influence the catalytic activity of gold structures, namely photo-activation, the size of the Au nanoparticles, the Au-support interactions, as well as the use of ligands or other surface modifiers.^[15] While the prowess of gold in hydrogenation reactions is clearly shown, several challenges remain. One is the agglomeration of particles on the support, which renders the catalyst inactive. Yet another important issue is the incorporation of hetero-atoms, which could lead to increased catalytic activity. Moreover, it is again stated that a thorough understanding of the structure of the catalyst is of paramount importance to design of the catalytic system.^[15]

Gold Nanoclusters for Hydrogenation Reactions

Considering these findings, it is plausible to look for a material that has a definite structure, which properties can be tuned to fit different purposes and that shows improved catalytic properties. Atomically precise gold nanoclusters, have been shown to be excellent candidates for catalysing hydrogenation reactions^[14, 36–38].

In their recent study, Wan and co-workers investigated the effect of the ligands on the catalysis of gold nanoclusters.^[38] For this purpose, they synthesized two isostructural nanoclusters, with different ligands, allowing them to specifically study the effect of this parameter on the catalysis. It was found that the different ligands disrupt the electronic configuration of the cluster, thereby giving different catalytic activities. While one cluster showed almost complete conversion, the other was almost inactive.^[38] This account shows the important role the ligands play in designing the catalyst.

A recent review from the Jin group summarized the size-effect of gold nanoclusters in catalysis.^[39] According to this account, there are several factors weighing in on this effect, namely the surface area, the surface geometry and the electronic structure of the nanoclusters. Generally speaking, smaller structures will have a larger specific surface area, leading to more active sites, allowing for improved catalytic activity. However, when multiple clusters of similar dimensions behave differently in catalytic reactions, this could be an indication for the geometric factor. Due to their small size, nanoclusters do not form facets, as would be expected from nanoparticles, leaving only corner- or edge-like sites available. Moreover, it is known that changing even only one atom in such structures can vastly change their geometry, hereby altering their catalytic properties. Another aspect to consider is the electronic structure of nanoclusters, which is, in contrast to bulk and nanoparticles, quantised.^[39]

Furthermore, another important factor to consider in heterogeneous catalysis is the support of the catalyst. It has been shown, that different supports interact differently with the catalyst and these interactions are paramount for the catalytic process.^[39] Generally, supports can be divided into two groups, namely inert and active supports. In thermocatalysis, commonly used inactive supports are, for example Al_2O_3 and SiO_2 . While such supports only help disperse the nanoclusters and immobilize them, others such as CeO_2 , interact with nanoclusters more strongly, thereby having a direct effect on the catalytic activity.^[40] A recent work done by the Barrab s group^[40] showed that upon pretreatment, the structure of gold nanoclusters changes, with parts of the cluster migrating to the surface of support, where new structures are created.^[40] This goes to show that not only the support, but also the pretreatment of the catalyst greatly influences the catalytic process.

A recent work by Barrab s group revealed interesting correlations between the choice of ligand, support and pretreatment in the semihydrogenation of phenylacetylene.^[41] It was reported that a reductive pretreatment had a positive effect on the catalytic activity and that the acid/base properties of the supports impacted on the catalysis, likely due to the stability of the clusters on the support.^[41] Considering the preliminary results showed there, it seemed plausible to further investigate this system and the influence of the different parameters. A scheme of supported nanoclusters, more specifically, of the ones that are used in this thesis, is presented in Figure 1.4.

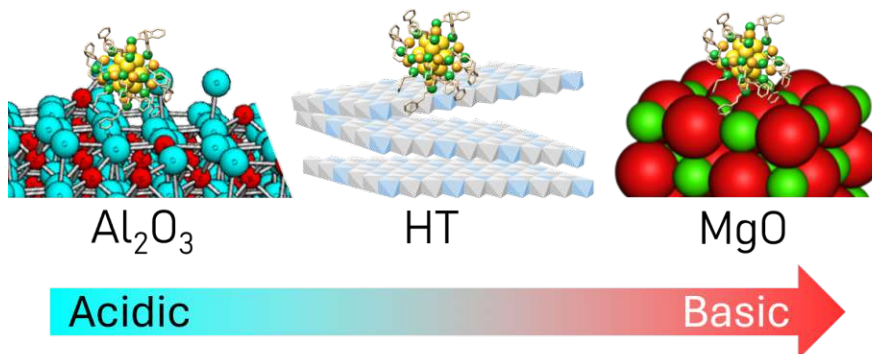


Figure 1.4.: Scheme of supported nanoclusters.

1.3. Reduction of Ketones to Alcohols

In order to get a complete picture of how nanoclusters behave in catalysis, it was deemed suitable to not only study them in heterogeneous catalysis, but also in a homogeneous system. In this way, the effect of the cluster itself, unaided or hindered by supports, could be investigated. To this end, the reduction of ketones to alcohols was chosen as a model reaction, more specifically, the reduction of acetophenone to 1-phenylethanol. The reaction scheme is displayed in Figure 1.5. As previously mentioned, the hydrogenation of ketones is prevalent especially in the pharmaceutical industry, due to its importance in the synthesis of various drugs.^[6-8]

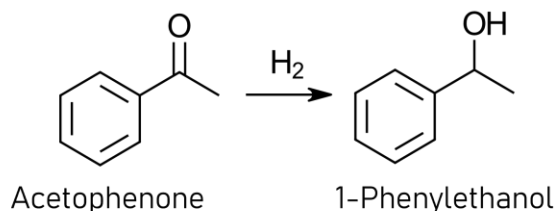


Figure 1.5.: Scheme of the reaction investigated in homogeneous catalysis.

1.3.1. Current Works

Currently, the catalysis in this field revolves around biocatalysts and organic catalysts. However, as is generally the case with such systems, the catalysts are often highly substrate specific, not allowing for broad application and are also quite complex and problematic to synthesize. Nevertheless, several works have been done, exploring ways to solve these issues.

Koesoema and co-workers recently published a mini-review, summarizing the work done with alcohol dehydrogenases, as catalysts in the reduction of carbonyl compounds to their corresponding alcohols.^[8] One great advantage of such compounds is their wide substrate

compatibility, allowing them to be used in a variety of reactions.^[8] A recent study by Karume and co-workers showed that, for example, alcohol dehydrogenases can also be used in non-biological settings, by immobilizing them using the so-gel method and using them in organic solvents^[42]. A different approach employing biocatalysts is that of using ketoreductases. In a recent report, Huang and co-workers showed that pro-chiral ketones could be converted to alcohols containing more than one chiral center, by using ketoreductase catalysts. While the approach seems promising, several challenges remain, as for example the complexity of the process.^[6]

Other works focused on the use organic compounds as catalysts. Kawanami *et al.* used oxazaborolidine for the reduction of a variety of ketones.^[7] They were able to generate these structures *in-situ* and showed that they are highly active and selective with a multitude of substrates. Furthermore, they were able to provide more reproducible results as other works with such materials, by improving the stability of these compounds.^[7]

1.3.2. Gold nanoclusters in Ketone Reduction

While bio- and organic catalysts are currently very popular for ketone reductions, inorganic catalysts are drawing more and more attention, due to their more facile synthesis and wide applicability. In this sense, there have also been a few works with gold nanoclusters, for the reduction of α – and β – *unsaturated* ketones to their corresponding alcohols.^[43, 44] Zhu *et al.* used gold nanoclusters in order to catalyse the reduction of such ketones in homogeneous system, with reported 100 % selectivity.^[43] Furthermore, some theoretical work by Ouyang and co-workers gave some insights into the mechanism of the reaction.^[44] They found that there are strong interactions not only between the cluster and the substrate, but also with the solvents. It was reported that the hydrogen cleaves and forms a hydride on the gold surface and that the solvent helps stabilize the substrate intermediate.^[44]

These results present important first steps in placing gold nanoclusters on the radar as potential catalysts for ketone reduction. Starting from this many opportunities can be explored, which is why the second part of this thesis aimed to expand on this work by employing nanoclusters of different sizes and with different ligands in the homogeneous hydrogenation of acetophenone.

2. Motivation of the Thesis

Hydrogenation reactions are important for multiple industries. In this thesis, the semi-hydrogenation of alkynes and the reduction of ketones will be studied. As previously described, such reactions are well documented and several opportunities for catalysis have been explored. However, a true understanding of the catalytic process at an atomic level is missing. Due to the complexity of the current catalysts, it is impossible to understand all contributing factors that lead to an efficient catalytic process, making the optimisation of the catalyst difficult. Because of this, an atomically precise, highly tuneable material is desirable, as this would allow for a controlled study of the different structural factors of the catalyst, allowing for a deeper understanding of catalysis.

Gold nanoclusters are a novel class of atomically precise materials, which have been shown to be active in various catalytic reactions. Because of their atomic definition and specific structure, it is possible to tune their properties individually. When used in catalysis, either in homogeneous systems or supported on metal oxides as heterogeneous catalysts, it is possible to individually change aspects of their structure and investigate the effect this has on the catalysis, thereby understanding the reason for certain trends and allowing for better catalyst optimisation.

This thesis aims to study the use of gold nanoclusters in both homogeneous and heterogeneous systems and understand the different factors that contribute to the catalytic activity. The goal is to design highly active and selective heterogeneous catalysts for the semihydrogenation of alkynes, a reaction that is of high importance for the petrol industry. Moreover, the influence of the support, pretreatment and ligands should be investigated. Furthermore, in order to gauge the influence of the different parts of the cluster structure, clusters of different sizes and slightly different configurations are tested in the homogeneous reduction of ketones to alcohols. Hereby, the influence of size and staple configuration should be explored, so that a complete picture of the influence of all structural components can be made.

3. Experimental Section

3.1. Experimental

3.1.1. Materials

The reagents, solvents and other consumables used in the preparation of nanoclusters were obtained from commercial suppliers. Any steps involving aqueous solutions were performed using ultrapure Milli-Q H₂O (18.2 MΩ · cm at 25 °C).

Hydrogen tetrachloroaurate trihydrate, H₂AuCl₄ · 3 H₂O (≥49.0 % Au basis), sodium tetrahydroborate, NaBH₄ (98 %) and triphenylphosphine (≥99 %) were obtained from Alfa Aesar. Tetraoctylammonium bromide, TOABr (≥98 %) was ordered from TCI Chemicals. 2-phenylethanethiol (98 %) and phenylacetylene (98 %) were purchased from Sigma Aldrich. Pyridine (ACS, Reag. Ph Eur) was acquired from Supelco. HPLC grade ethanol and toluene were purchased from Carl Roth. Milli-Q water (resistivity of 18.2 MΩ · cm at 25 °C) was used in the synthesis procedure. All solvents used (dichloromethane, methanol, tetrahydrofuran, toluene, etc.) were at least of synthesis grade and used without further purification. Bio Beads S-X1 support (Bio-Rad) was used for size exclusion chromatography (SEC).

3.1.2. Nanocluster Synthesis

Au₁₁(PPh₃)₇Br₃

The cluster was prepared according to a previously reported protocol by Truttmann *et al.*^[45] A solution of H₂AuCl₄ · 3 H₂O (1 eq., 501 mg, 1.27 mmol) and TOAB (1.2 eq., 833 mg, 1.52 mmol) were dissolved in 50 mL THF in a round bottom flask, forming an orange solution. Subsequently, triphenylphosphine (5 equiv., 1162 mg, 6.34 mmol) was added, whereupon a colorless mixture was obtained. The solution was allowed to stir for 1 h at room temperature, followed by the addition of NaBH₄ (10 equiv., 474 mg, 12.54 mmol) dissolved in 10 mL cold Milli-Q water.

The reaction mixture was stirred for 48 hours, resulting in a dark brown precipitate. After evaporation of the solvent under reduced pressure, the remaining solid was washed with a 1:1 mixture of MeOH:H₂O. Then, the by-products were extracted with THF, toluene, and a 2:1 mixture of hexane:EtOH, respectively. Each solution was analyzed *via* UV-Vis. The Au₁₁ cluster was extracted with DCM, showing two prominent bands. Upon evaporation of the solvent an orange solid was obtained. The UV-Vis is shown in Figure 3.1.

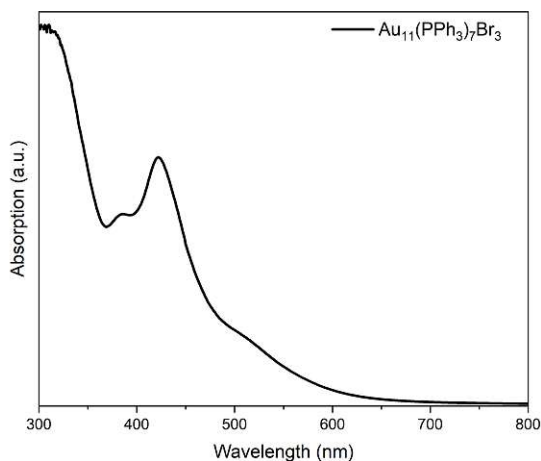
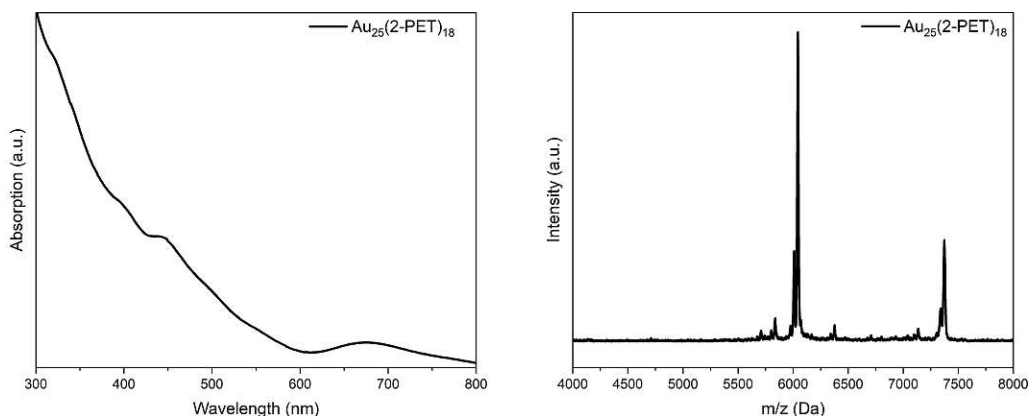


Figure 3.1.: UV-Vis spectrum of the pure $\text{Au}_{11}(\text{PPh}_3)_7\text{Br}_3$ nanocluster.

$\text{Au}_{25}(\text{2-PET})_{18}$ and $[\text{Au}_{25}(\text{2-PET})_{18}]^-\text{TOA}^+$

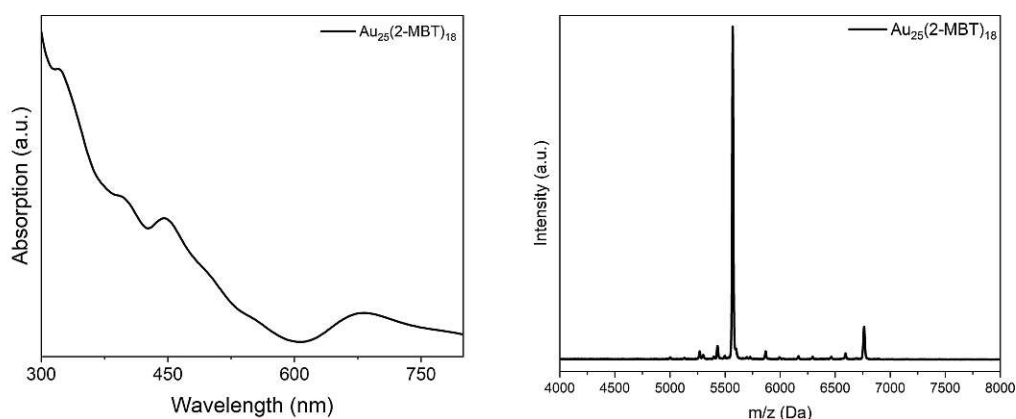
The cluster was synthesized following previous experience.^[46] To begin with, TOABr (1.2 eq., 833 mg, 1.52 mmol) and $\text{HAuCl}_4 \cdot 3 \text{H}_2\text{O}$ (1 eq., 500 mg, 1.27 mmol) were dissolved in 50 mL THF, after which 850 μL of 2-PET were added, whereupon the color of the orange solution faded out after stirring for 1 h. Then, 480 mg of NaBH_4 in 10 mL cold Mili-Q water were added. The mixture was stirred at room temperature for 4 days. Upon evaporation of THF, the precipitate was repeatedly washed with a 1:1 mixture of water in methanol and then with pure methanol. The crude product was extracted with acetone and purified *via* SEC, yielding a black solid. The UV-Vis and MALDI-MS spectra of the pure product are shown in Figure ??.



(a) UV-Vis spectrum of the pure $\text{Au}_{25}(\text{2-PET})_{18}$ (b) MALDI-MS spectrum of the pure $\text{Au}_{25}(\text{2-PET})_{18}$ nanocluster.

Au₂₅(2-MBT)₁₈ and [Au₂₅(2-MBT)₁₈]⁻TOA⁺

Au₂₅(2-MBT)₁₈ and [Au₂₅(2-MBT)₁₈]⁻TOA⁺ were synthesized following literature.^[46, 47] To a 10 mL THF solution of 200 mg (0.25 mmol) HAuCl₄ · 3 H₂O and 167 mg (0.31 mmol) TOAB, 156 μL (1.27 mmol) of 2-MBT were added, which resulted in the original orange color of the solution slowly fading out over the course of an hour. The reaction mixture was then reduced by addition of 96 mg (2.54 mmol) NaBH₄ in 2 mL ice-cold Milli-Q water. Stirring at room temperature was continued for 2 days, after which the solvent was removed by rotary evaporation and the residue washed with 1:1 water:methanol and purified by SEC (THF/Bio-Beads S-X1 support). After elution of a black fraction (which was identified as Au₁₄₄(2-MBT)₆₀), a reddish-brown fraction of [Au₂₅(2-MBT)₁₈]⁻TOA⁺ and a greenish fraction containing Au₂₅(2-MBT)₁₈ could be isolated. The UV-Vis and MALDI-MS spectra of the pure clusters are depicted in Figure ??.

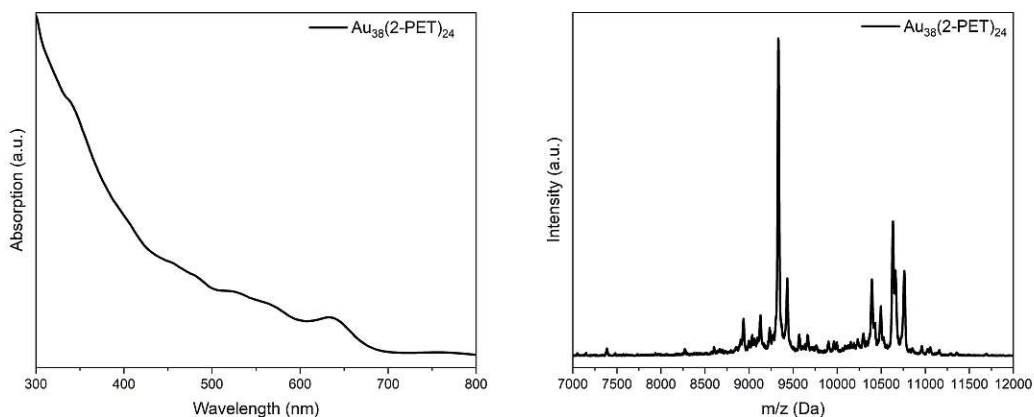


(c) UV-Vis spectrum of the pure Au₂₅(2-MBT)₁₈ (d) MALDI-MS spectrum of the pure Au₂₅(2-MBT)₁₈ nanocluster.

Au₃₈(2-PET)₂₄

Au₃₈(2-PET)₂₄ was synthesized according to previous experience.^[46] To begin with, 1 g (2.9 mmol) of HAuCl₄·3H₂O was mixed with 3.17 g (10.3 mmol) of *L*-glutathione (GSH), and dissolved in 100 ml of acetone, to yield a yellow suspension (Au-SG polymers). The mixture was stirred at 0 °C for 30 min, after which a cooled solution of 30 ml Milli-Q grade water and 0.98 g (0.0259 mol) NaBH₄ was slowly added. This resulted in the formation of a black precipitate (Au_n(SG)_m clusters). The solvent was then decanted and the solid dried at 100 mbar and room temperature. Subsequently, 6 ml of EtOH, 10 ml of toluene, 30 ml of Milli-Q grade water, and 10 ml (74.7 mmol) of 2-PET were added. The mixture was stirred for 4 h at 80 °C. After cooling the reaction mixture to room temperature, 50 ml of hexane were added, yielding a clear organic phase. The black precipitate was filtered and washed several times with MeOH. Following this, the crude product was extracted with DCM and dried at reduced pressure at 30 °C. The crude product was purified by size exclusion chromatography (SEC) with THF as mobile phase and Biobeads SX-1 support (company Bio-Rad) as stationary phase.

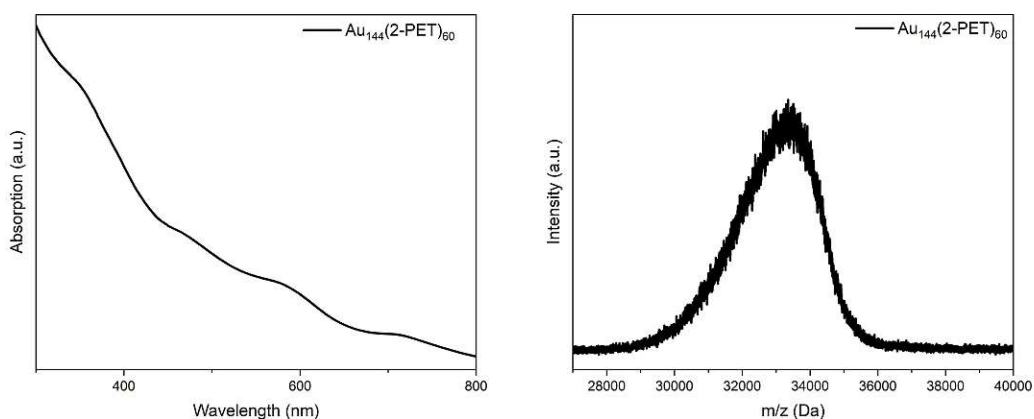
The size and purity of the obtained clusters was determined by UV-Vis spectroscopy in DCM and MALDI-MS, with the spectra depicted in Figure ??.



(e) UV-Vis spectrum of the pure $\text{Au}_{38}(\text{2-PET})_{24}$ (f) MALDI-MS spectrum of the pure nanocluster. $\text{Au}_{38}(\text{2-PET})_{24}$ nanocluster.

$\text{Au}_{144}(\text{2-PET})_{60}$

$\text{Au}_{144}(\text{2-PET})_{60}$ was synthesized according to a previously reported synthesis.^[48] To begin with, 18 mg (0.3 mmol $\text{HAuCl}_4 \cdot 3 \text{H}_2\text{O}$ and 190 mg (0.348 mmol) TOAB were dissolved in 15 mL methanol and stirred for 15 min at room temperature, whereby the solution turned from yellow to dark red. Subsequently, 0.213 mL (1.59 mmol) 2-PET were added, yielding a white suspension, which was stirred for 15 min. Afterwards, a fresh solution of NaBH_4 (3 mmol in 6 mL of ice cold Milli-Q water) were rapidly added, resulting in the formation of a black precipitate. The reaction mixture was stirred for 5 h at room temperature. Next, the precipitate was collected by centrifugation and washed several times with methanol. Finally, the crude product is extracted with DCM and purified by SEC. The UV-Vis and MALDI-MS spectra of the pure clusters can be seen in Figure ??.



(g) UV-Vis spectrum of the pure $\text{Au}_{144}(\text{2-PET})_{60}$ (h) MALDI-MS spectrum of the pure nanocluster. $\text{Au}_{144}(\text{2-PET})_{60}$ nanocluster.

3.1.3. Preparation of supports

The α - Al_2O_3 was procured commercially from abcr GmbH. The hydrotalcite was synthesized according to literature^[41] by another member of the group. To this end, the co-precipitation method was applied. A mixture of $\text{Mg}(\text{NO}_3)_2$ and $\text{Al}(\text{NO}_3)_3$ of acidic pH was mixed with a basic one of NaOH and NaNO_3 , whereby the reactants were chosen such as to obtain a molar ratio of 4 of Mg:Al. The solutions were mixed drop-wise at room temperature and standard pressure, using an infusion pump with a flow of 1 mL/min. Following this, the solution was aged at 60 °C for 24 h, after which the solid was filtered and washed with water until a pH of 7 was reached. Finally, the HT was dried at 100 °C for 24 h. The MgO was also prepared by another member of the group, according to previous experience^[41]. In this case, 25 g of $(\text{MgCO}_3)_4\text{Mg}(\text{OH})_2$ were suspended in 750 mL of water and stirred at 80 °C for 30 min, after which the solid was filtered and dried at 90 °C for 24 h, followed by calcining at 450 °C for 2 h.

3.1.4. Preparation of supported nanoclusters

Both Au_{25} and Au_{11} were supported on all three metal oxides, with a metal loading of 0.05 wt% following the same protocol. The appropriate amount of nanocluster was dissolved in HPLC grade toluene or ethanol respectively, and mixed with a suspension of the metal oxide in the same solvent. The mixture was then stirred for 24 h at room temperature, after which the now clear solvent was slowly removed under reduced pressure. The obtained powder was dried in an oven at 80 °C for 1 h, after which parts of it were pretreated by calcining in an oven at 150 °C and 250 °C for 1 h, heating at a rate of 10 °C/min.

3.1.5. Catalytic tests

Heterogeneous System

The catalytic tests were performed in an autoclave, at 8 bar H_2 and 100 °C. The reactor was purged three times with hydrogen before the final filling. 2 mg of catalyst, 0.08 mL pyridine, 0.11 mL phenylacetylene and 2 mL of ethanol were reacted for 24 h at the specified temperature and pressure, in batches of six. The samples were filtered using syringe filters and the solution analyzed by gas chromatography (GC).

The quantification was done by external calibration on GC, on a Shimadzu GC-2014, equipped with a Flame Ionization Detector (FID) and a HP-5 column of 30 m length, 0.25 μm film thickness and 0.32 mm column ID. For each injection, the syringe was rinsed three times with solvent, followed by rinsing three times with sample and after the injection, another three solvent rinses. 1 μL of sample was injected for each measurement and each sample was measured three times. The initial temperature of the GC was held at 60 °C for 7 min, followed by heating up to 250 °C with a ramp of 50 °C/min and a holding time of 2 min. The oven temperature was 60 °C, the injection chamber was held at 250 °C and the FID at 300 °C. The measurements were done in Split mode, with a split of 18:100, a column flow of 2.49 mL/min and a total flow of 50.1 mL/min.

The peaks were integrated by hand and the the areas converted to concentrations using the linear regression obtained from the external calibration. The conversion (X) and selectivity (S) were calculated according to the following formulae. The yield was calculated by dividing the selectivity by the conversion. The calibration lines can be found in the Appendix.

$$X = \frac{c_{PA,0}}{c_{PA}} \cdot 100$$

$$S_i = \frac{c_i}{\sum c_i} \cdot 100$$

Homogeneous System

The catalytic tests were performed in the same autoclave as the heterogeneous reactions. The conditions were 8 bar H₂, temperature ranging from 25 °C to 40 °C, time of 24 h, with 1 mg of cluster catalyst, in 0.1 mL toluene and 1.9 mL iPrOH, with 432 μ L Acetophenone as substrate. The samples were then analysed by HPLC. A qualitative calibration was performed by measuring standards of all compounds contained, as well as the expected product, 1-phenylethanol. The quantification of the conversion was achieved, by relating the area of the precursor before and after the reaction. The integration of the peaks was done automatically by the analysis program. A chromatogramms containing each compound can be found in the Appendix.

The analysis was done on a Shimadzu LC-20AD HPLC equipped with a DGU-20A5R degassing unit, a SIL-20AHT autosampler, SPD-20A UV-Vis detector and a CBM-="A communications bus module. The column used was a Phenomenex Lux 5 μ m *i*-Amylose-1 column. Following a method development where multiple flow rates and solvent mixtures were tried, a flow of 1 mL/min and a hexane:iPrOH ratio of 95:5, as well as a detection at 265 nm were chosen.

3.1.6. X-Ray Absorption Fine Structure (XAFS) Spectroscopy

XAFS is a powerful characterization technique, giving insights about the electronic state of the elements in a compound and about the structural arrangement of said atoms. The spectrum is split in two sections, the X-Ray Near Edge Absorption Spectroscopy (XANES) and the Extended X-Ray Absorption Fine Structure Spectroscopy (EXAFS). While the XANES delivers information regarding the oxidation state of the atoms, the EXAFS region offers insights into atomic distances and coordination numbers. This complementary information allows the user to study the sample thoroughly and for example investigate the way different outside factors impact on the structure.^[49]

XAFS measurements were performed at the CLAES Beamline at Alba Synchrotron in fluorescence mode (Au-L₃ edge and S-K edge) in the beamline's sample holder for static measurements. The catalysts were pressed into pellets and secured by kapton tape.

The synchrotron radiation emitted by a wiggler source was monochromatized using a double crystal Si(311) monochromator. The rejection of higher harmonics was done by choosing

proper angles and coatings of the collimating and focusing mirrors. XAS measurements were performed in fluorescence continuous mode using a multielement silicon drift detector with Xspress3 electronics. Slit gap in front of IO ionization chamber have been set to different values in order to guarantee the correct deadtime values depending on the sample measured. Energy scale at Au-L₃ and S-K edges have been previously calibrated by measuring the Au and S foils respectively.

The raw spectra have been processed by other parties according to standard methods. They have been normalized by approximating pre-edge and post-edge backgrounds are low-order polynomial curves. The corresponding EXAFS signal has been then extracted, k-squared weighted, and Fourier transformed (FT). The fresh, untreated samples have been used as starting points for all EXAFS modelling, providing the theoretical phases and amplitudes of the scattering paths by means of self-consistent ab-initio calculations performed with FEFFlite code^[50]. Furthermore, in order to get more conclusive structural parameters from the EXAFS, all spectra were fitted on the Au-L₃ edge using a personalized code based on IFEFFIT^[51].

Two two shell models were considered for fitting the data (with Au-Au and Au-S or Au-P contributions). As fitting parameters, the coordination numbers CN $N_{\text{Au-Au}}$, $N_{\text{Au-S}}$ and $N_{\text{Au-P}}$, as well as three correction factors for the inter-atomic distances $\Delta R_{\text{Au-Au}}$, $\Delta R_{\text{Au-S}}$ and $\Delta R_{\text{Au-P}}$. Furthermore, three disorder parameters were used, $\sigma^2_{\text{Au-Au}}$, $\sigma^2_{\text{Au-S}}$, $\sigma^2_{\text{Au-P}}$. The following table lists the fitting parameters for both systems. The figures corresponding to the fitting can be found in the Appendix.

Table 3.1.: Fitting parameters for the EXAFS spectra.

amp	Enot(Au)	Enot(Au-S)	Enot(Au-P)	$\sigma^2_{\text{Au-Au}}$	$\sigma^2_{\text{Au-S}}$	$\sigma^2_{\text{Au-P}}$
0.92 ± 0.22	3.73 ± 1.09	2.64 ± 1.62	8.33 ± 3.63	0.009 ± 0.002	0.005 ± 0.001	0.013 ± 0.003

3.1.7. Characterization

Ultraviolet-Visible Spectroscopy

Nanoclusters have a fingerprint spectrum that allows for almost concrete identification of the different species, which is why this technique is the go-to method for preliminary characterization. UV-Vis spectroscopy was performed on a UV-1600PC spectrometer using cuvettes of 1 cm pathlength. Different solvents (DCM, toluene, THF) were used to dissolve the Au nanoclusters.

Matrix-assisted Laser Desorption/Ionization (MALDI-MS)

While UV-Vis gives preliminary information about the purity of the nanoclusters, mass spectrometry is the final confirmation, as even differences in ligands can be seen here. Matrix-assisted laser desorption/ionization mass spectrometry (MALDI-MS) was conducted on a Bruker Ultraflex extreme MALDI-TOF instrument equipped with a Nd:YAG laser in linear

mode. Each spectrum was obtained by averaging 5000 single shots (split in packets of 500 shots). Spectra were obtained at 10 % laser power. trans-2-[3-(4-tert-Butylphenyl)-2-methyl-2-propenyliden]-malononitrile (DCTB) was used as matrix. Sample and matrix solutions were prepared in toluene.

X-Ray diffraction (XRD)

Powder X-ray diffraction (XRD) was performed using a PANalytical X'Pert powder diffractometer in Bragg-Brentano geometry. The diffractometer was equipped with a Cu LFF X-ray tube operated at 45 kV and 40 mA (Cu K_{α}), a BBHD mirror, and a Malvern PANalytical MPD Pro (PW3050/60 goniometer) with 200 mm goniometer radius. The 2θ ranges were set between 4,99 to 128° with a step size of 0.02°.

4. Results and Discussion

4.1. Heterogeneous Semihydrogenation of Alkynes

The support, ligand and pretreatment effects on the activity and selectivity of gold nanoclusters was investigated in the semihydrogenation of phenylacetylene in liquid phase. For this purpose, two kinds of clusters were synthesized: $\text{Au}_{11}(\text{PPh}_3)_7\text{Br}_3$ and $\text{Au}_{25}(\text{SC}_2\text{H}_4\text{Ph})$. Details about their synthesis and characterization can be found in the Experimental Chapter. Due to their different ligands, the clusters have disparate structures. The Au_{11} , a phosphine protected cluster, consists of a gold core on which the phosphines are directly bound. On the other hand, the Au_{25} cluster, which is thiolate protected, has a more complex structure. In the case of thiolate protected gold nanoclusters, the ligands are attached to the core through -S-Au-S-Au-S- oligomers, also called staple units, as described in the Introduction. The structures of these nanoclusters are presented in Figure 4.1. For the catalytic tests, the clusters were supported on three different metal oxides, Al_2O_3 for its acidity, MgO for its basicity and a hydrotalcite (HT), which is a layered oxide composed of Al_2O_3 and MgO , with a neutral pH. Details on the supporting procedure and metal loading can be found in the Experimental Chapter. Previous works have shown that the pretreatment of such catalysts can have a significant effect on their catalytic performance, due to the ensuing of temperature dependent ligand stripping.^[52, 53] In order to investigate this, the catalysts were calcined at 150 °C and 250 °C (details in Experimental). This led to a total of six different catalysts, with two additional pretreated versions each, which were employed in condensed phase catalytic tests. In the following, the catalysts will be referred to as 11Al, 11Mg, 11HT, 25Al, 25Mg and 25HT.

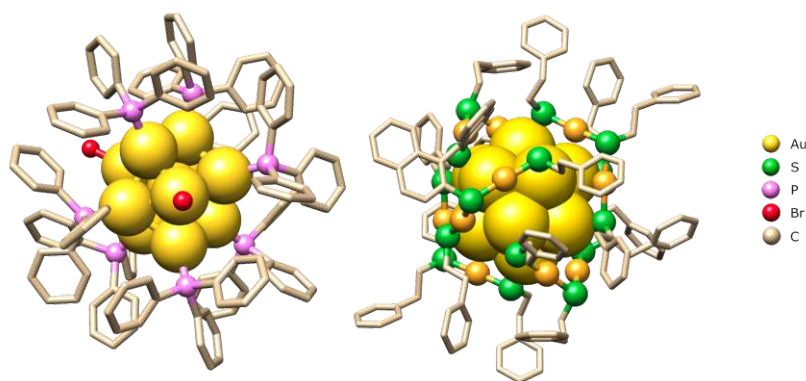


Figure 4.1.: Structure of the synthesized nanoclusters.

4.1.1. Catalytic Activity

The analysis of the catalytic tests was done by GC, as described in the Experimental Section, together with information about the calibration. Significant differences were observed in the activity of the nanoclusters, depending on their support, ligands and pretreatment. In the case of the supported Au₁₁ nanoclusters, the 11Mg showed the highest conversion, as can be seen in Figure 4.2. Without pretreatment and by pretreating at 150 °C, the catalyst showed similar levels of activity, close to 50 %. After pretreatment at 250 °C however, the conversion rose to 98 %. In comparison, the other Au₁₁ catalysts showed a maximum conversion of 36 %. The yield of styrene is presented in Table 4.1.

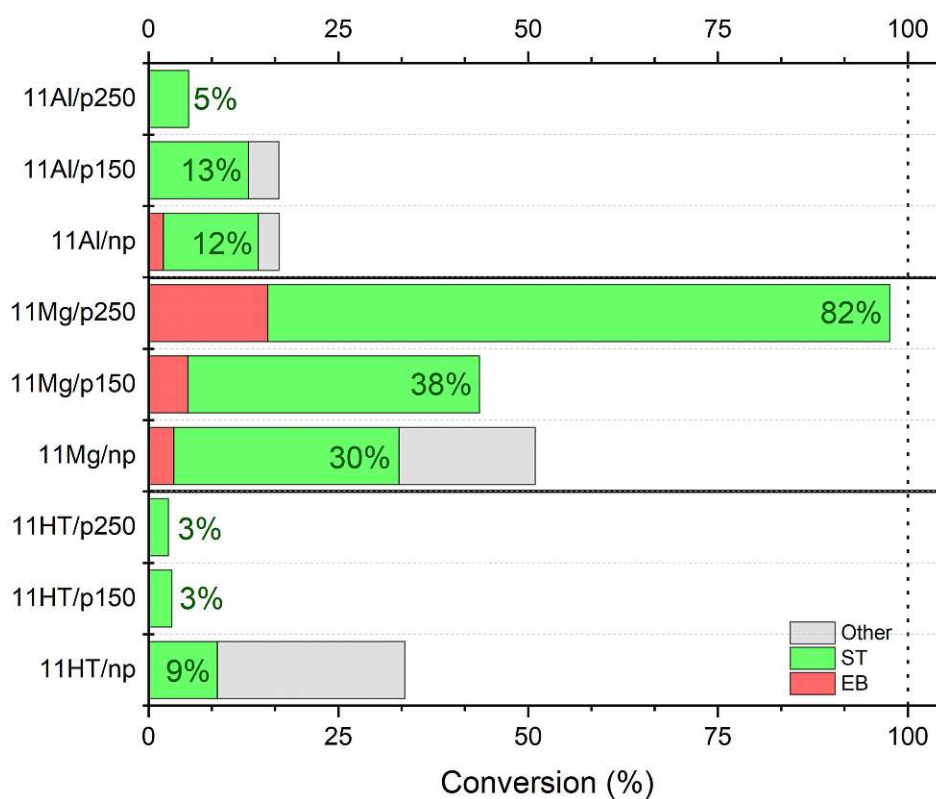


Figure 4.2.: Conversion of phenylacetylene is represented by the total height of the bar. The different colors represent the selectivity of the Au₁₁ catalysts toward styrene (ST), ethylbenzen (EB) and other side-products (Other). The level of pretreatment is indicated by the abbreviations next to the catalyst name, with *np* meaning no pretreatment, *p150* referring to pretreatment at 150 °C and *p250* at 250 °C.

When looking at Figure 4.2, it seems that in this case, the reaction favors the basicity of the MgO support, corroborating previous reports, that hypothesized that basic sites facilitate the cleavage of H₂^[41]. Furthermore, the increase in activity after pretreating at 250 °C indicates a change in the cluster's structure. According to previous experience, pretreating the supported

clusters strips the ligands, exposing the gold core to the reactants, thereby creating new active sites. This has to however be confirmed by XAFS spectroscopy. Furthermore, the selectivity of each catalyst is shown by the colors of the bars. While the activity of the catalyst increases, the selectivity towards the desired styrene (ST) decreases after pretreating to 250 °C, as more ethylbenzene (EB) is formed. This indicates that a balance has to be found between activity and selectivity. In order to increase activity, but retain the selectivity, it appears that the parameters of the reaction should be changed. A possible reason for the apparent decrease in selectivity could be the reaction time. Due to high almost complete conversion, it can be assumed, that after a certain reaction period, all present phenylacetylene is used up and converted to ST, after which the next possible reaction is the reduction of the ST to EB, thereby decreasing the selectivity. Considering this, it seems plausible that by decreasing the reaction time, the selectivity of the catalytic process can be improved.

The grey area representing other products can be attributed to polymerisation of ST, other oligomers being formed, or perhaps reactions between the substrate and the ligands.

Table 4.1.: Yield towards styrene of the Au₁₁ catalysts.

Catalyst	Yield (%)
11Al/p250	0,3
11Al/p150	2,3
11Al/np	2,1
11Mg/p250	80,0
11Mg/p150	16,7
11Mg/np	15,1
11HT/p250	0,1
11HT/p150	0,1
11HT/np	3,1

In the case of the supported Au₂₅ nanoclusters, a different trend is observed. In this case, the 25HT displays the highest activity and selectivity, as can be seen in Figure 4.3 (the yield towards ST is displayed in Table 4.2). Here, the 25HT/np showed the highest conversion with over 75 %. The pretreatment of this catalyst seems to have an inverse effect as compared to the Au₁₁ catalysts. The activity decreases with increased pretreatment temperature, but the selectivity increases. Therefore, in spite of the higher conversion rate of the 25HT/np, the 25HT/p150 is the more efficient catalyst, producing the same amount of ST without as many by-products. After pretreatment at 250 °C, the selectivity is best, but the activity is halved. This trend can be observed in the other catalysts as well.

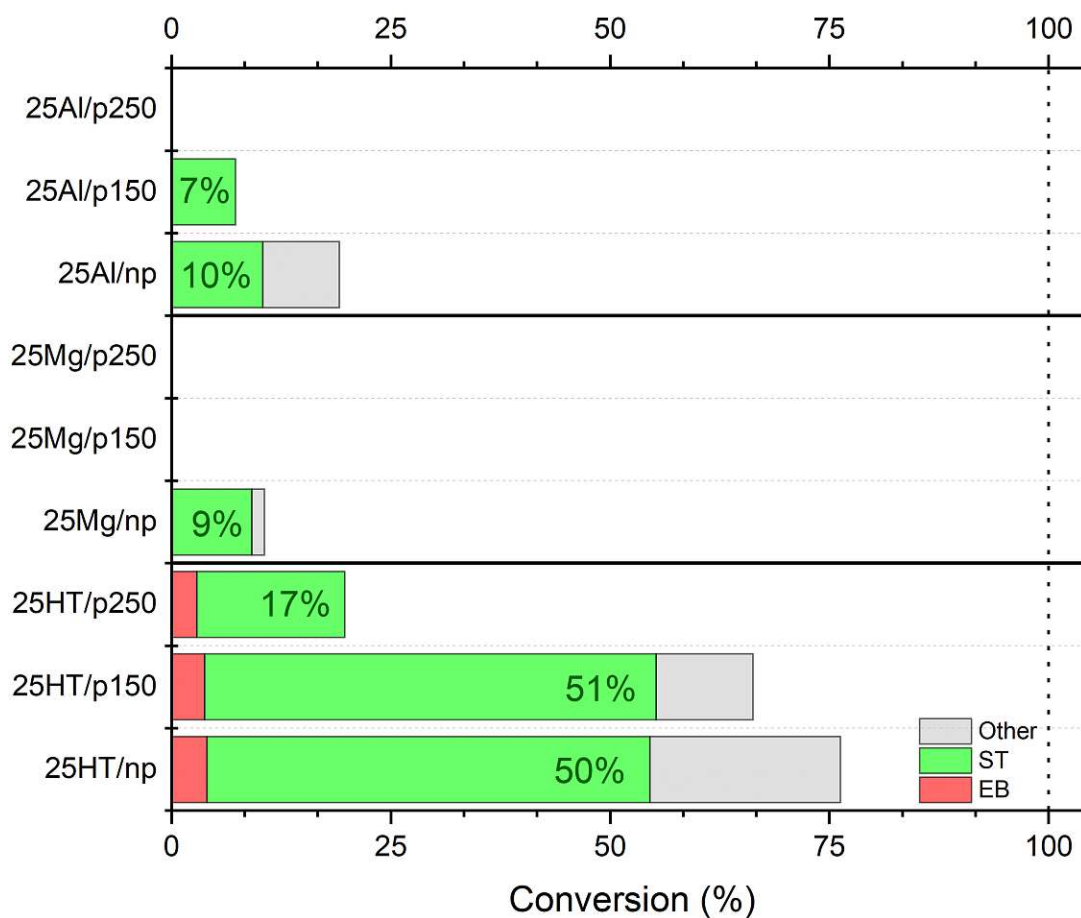


Figure 4.3.: Conversion of phenylacetylene is represented by the total height of the bar. The different colors represent the selectivity of the Au_{25} catalysts toward styrene (ST), ethylbenzen (EB) and other side-products (Other). The level of pretreatment is indicated by the abbreviations next to the catalyst name, with *np* meaning no pretreatment, *p150* referring to pretreatment at 150 °C and *p250* at 250 °C.

The different trend seems to be connected to the different type of ligands protecting the Au_{25} nanocluster. In contrast to the phosphine-protected Au_{11} , the thiolate-protected Au_{25} displays higher conversion without pretreatment, indicating that here, the ligands do play a role in the catalysis. This could be attributed to the different structure of the nanoclusters. In the case of the Au_{11} , the phosphine ligands are directly bound to the gold core. In the Au_{25} however, the thiolates are connected through staple units, as previously mentioned. The Au atoms in these oligomers are, in contrast to the metallic Au in the core, positively polarized. Therefore it can be hypothesized that the difference in the electronic structure has an impact on the catalytic process. Furthermore, because of the staple arrangement, more of the gold core is accessible for the activation of the hydrogen, which could explain the higher activity at lower pretreatment temperature. The decrease in activity could also be attributed to the interaction of the bared gold core with the present PA. Recent work by the Tsukuda

group found that PA can be used as a ligand for gold nanoclusters^[54]. Knowing this, it can be hypothesized that as the gold core is stripped of staples, PA binds as a ligand, thereby poisoning the active sites. Of note is also that the PA does not seem to bind to the gold in the Au₁₁ nanocluster, indicating that the different structure of the core plays a role in the ligand affinity. In order to confirm such assumptions however, XAFS studies are needed, as they would offer insights into the electronic structure of the catalysts.

Similarly to the Au₁₁ catalysts, some Au₂₅ also show strong production of other compounds. These could also be related to polymerisation of ST, formation of other oligomers, or reactions between the ligands and the substrate.

Table 4.2.: Yield towards styrene of the Au₂₅ catalysts.

Catalyst	Yield (%)
25Al/p250	0,0
25Al/p150	0,5
25Al/np	2,0
25Mg/p250	0,0
25Mg/p150	0,0
25Mg/np	1,0
25HT/p250	3,3
25HT/p150	34,1
25HT/np	38,5

In order to investigate the other products formed, as well as the effect of the support on the catalytic activity, catalytic tests were conducted with the pure supports, the free ligands, as well as a blank measurement containing no catalyst. The results are displayed in the chromatograms in the Appendix. The analysis of the blank showed 5 % loss of PA and no product formation, owing perhaps to evaporation during the reaction. This loss is however negligible, showing the robustness of the system. The measurement of the supports also showed little to no conversion, thereby showing that the catalysis happens due to the interaction of the substrate with the nanoclusters. Furthermore, the tests ran with the free ligands slightly increased levels of activity (16 % for the PPh₃ and 20 % for the 2PET) and no product formation. This could corroborate the hypothesis of the origin of some of the other products found in the reaction mixture, that could perhaps be due to interactions between the ligands and the substrate.

Considering the questions raised by the catalytic tests in regard to the interaction of the cluster with the support and the stability of the clusters during the reaction, several analyses needed to be conducted to address this. For this purpose, XRD of the two high performing catalysts, the 11Mg and 25HT, was performed, as well as XAFS spectroscopy of all catalysts.

4.1.2. Support Characterization

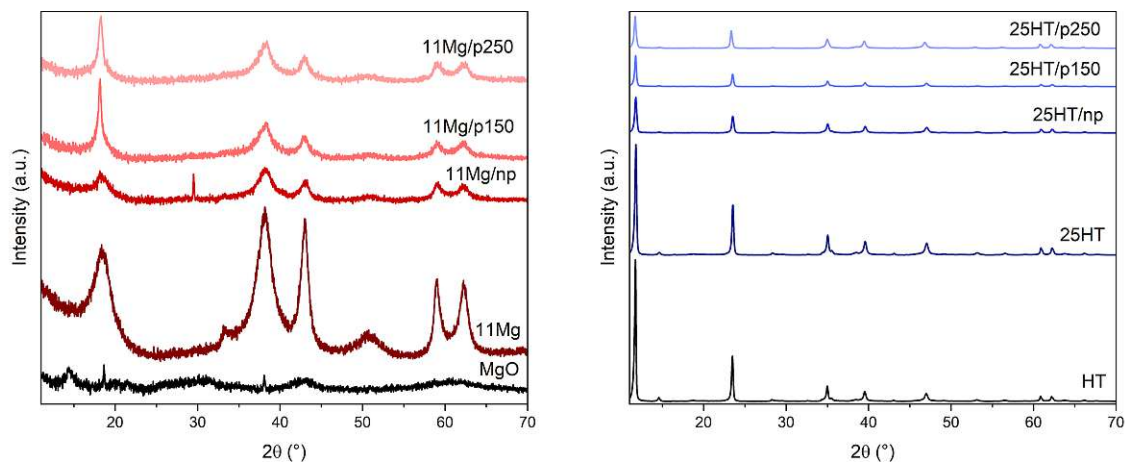


Figure 4.4.: XRD measurement of the 11Mg and 25HT catalysts, with the bare support as reference.

The XRD measurements of the 11Mg and 25HT catalysts are displayed in Figure 4.4, together with the bare support as reference. The lines displayed, other than the 11Mg and 25HT, correspond to the used catalysts. In the case of the catalysts supported on HT, a decrease in the crystallinity of the support can be observed, which gets stronger after the catalysts were used. This corroborates the hypothesized interaction of the catalyst with the support.

In the case of the catalyst supported on the MgO, the appearance of new peaks can be observed. When comparing this to literature^[55], it is apparent that the new peaks belong to $\text{Mg}(\text{OH})_2$. This again indicates a strong interaction of the cluster with the support. Furthermore, the intensity of the new peaks strongly decreases after the catalysts were used in the reaction. The formation of the hydroxide could be attributed to loss of ligands. On the other hand, considering the intensity of the peaks and the low metal loading used, the phenomenon seems to be unrelated to the cluster supporting. However, considering that the samples were stored in a freezer prior to the measurement, it could be possible that water entered the system, thereby producing the hydroxide and after the reaction took place, the water was removed due to the reaction conditions, thereby the decrease in the intensity of the peaks.

4.1.3. XAFS Analysis

In order to get more insight on the impact of the reaction conditions on the catalysts, XAFS measurements on the Au-L₃ and S-K edges were conducted at the ALBA synchrotron, on the CLAESS beamline. In order to gauge the influence on the electronic structure of the cluster, the XANES region of the spectrum was analysed and for investigating the influence on the structure.

XANES Analysis

In Figure 4.5, the XANES of the 11Mg catalysts can be seen, together with the spectra of the pure, unsupported Au_{11} cluster and the Au foil as references. The first observation to be made, is that there is no significant difference between the measured catalysts, regardless of the pretreatment, or reaction. It can be argued, that the white line (feature at 11 924 eV), slightly decreases in intensity, especially for the 11Mg/p150 - used and 11Mg/p250 - used samples, indicating that the cluster gets electronically closer to the metallic Au foil. Moreover, it can be seen, that all measurements neither match the Au foil, nor the unsupported cluster perfectly. This difference can be seen most strongly around the white line and can be attributed to the interaction of the cluster with the support, that could change the electron density around the gold atoms, thereby altering the electron structure of the cluster. Furthermore, the possible loss of ligands hypothesized after the analysis of the catalytic results, would also contribute to the change in intensity of the white line. This should however, be confirmed by EXAFS analysis. In the case of the feature at 11 945 eV, the resemblance to the pure cluster is much stronger, suggesting that the structure of the core itself is kept, as this band is generally representative also for structural information of the core. With the help of EXAFS however, more concrete speculations can be made.

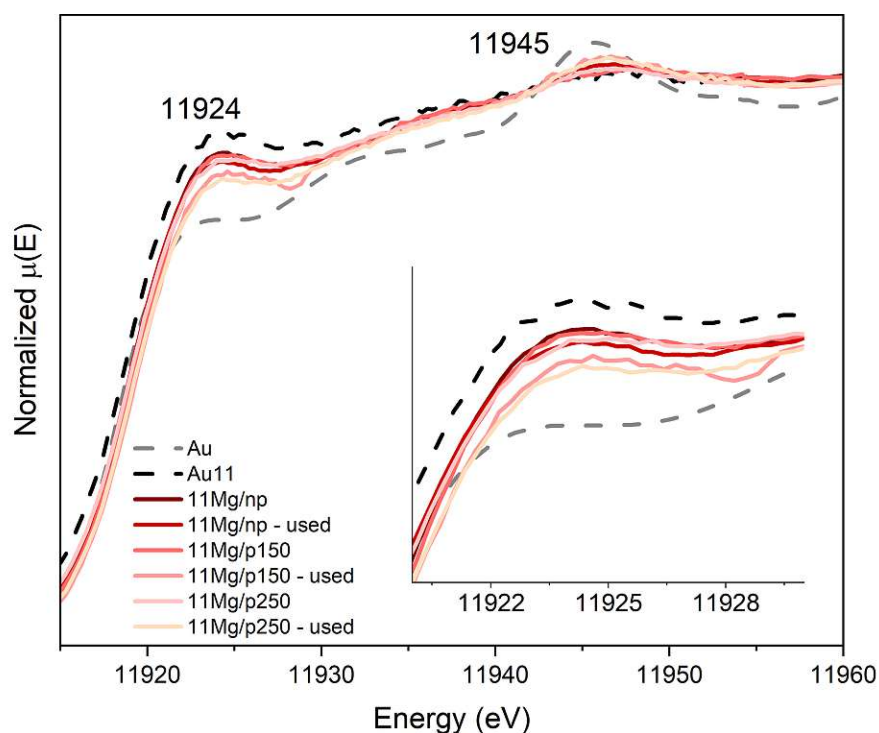


Figure 4.5.: XANES region of the XAFS spectrum of the 11Mg catalysts, together with the Au foil and the unsupported Au_{11} nanocluster as references.

In Figures 4.6 and 4.7, the measurements of the 11HT and 11Al catalysts are displayed. In the case of the 11HT catalysts, it can be seen that while the 11HT/np, 11HT/np - used and 11HT/p150 samples show a trend similar to the 11Mg catalysts, the rest of the samples appear to have altered electronic configurations, becoming almost identical to the metal foil. This can be corroborated to the catalytic test of these clusters, where it can be seen in Figure 4.2 that the untreated catalyst is near in conversion to the untreated 11Mg catalyst, although the selectivity towards ST is drastically lower. However, the other catalysts show almost no activity, which could be explained by the changes observed in the XANES. This further shows the importance of the support in the design of the catalyst, as it seems that there should be a different interaction of the cluster with the HT, that does not lend it such a high stability as the MgO. In the case of the 11Al catalysts, the XANES of the fresh sample shows good correlation with the unsupported cluster, indicating that the supporting was successful however, as soon as the cluster is employed in the reaction, it appears that the electronic properties are changed and now samples looks almost identical to the Au foil. This could explain the lack of conversion of these catalysts, as presented in Figure 4.2. It can thus be concluded that Al_2O_3 is also not a suitable support for nanoclusters in this reaction, perhaps owing to its acidic character.

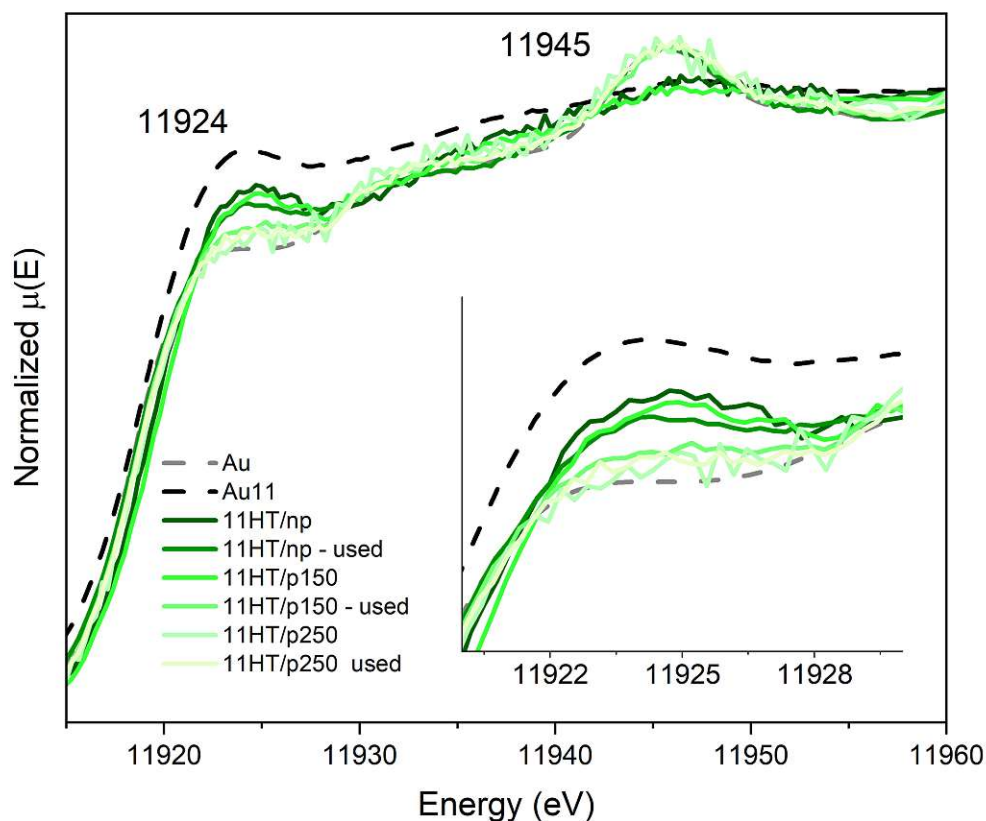


Figure 4.6.: XANES region of the XAFS spectrum of the 11HT catalysts, together with the Au foil and the unsupported Au₁₁ nanocluster as references.

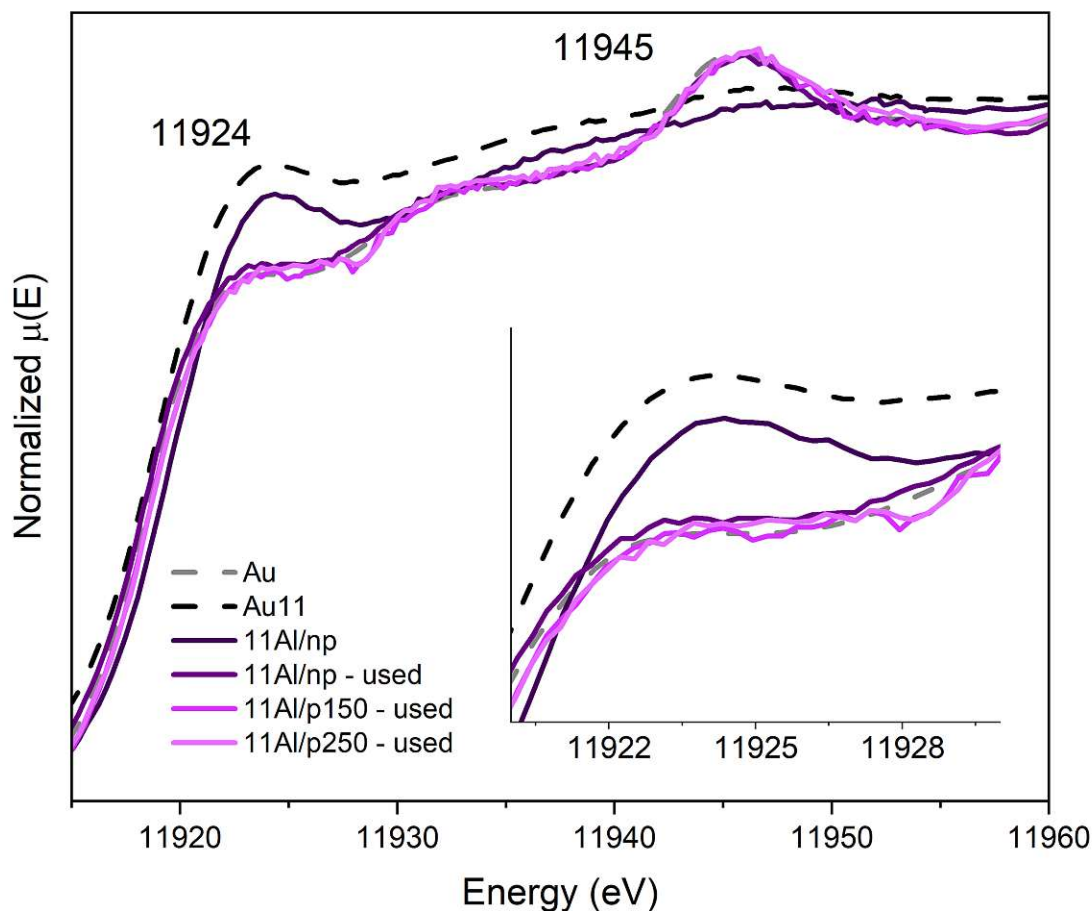


Figure 4.7.: XANES region of the XAFS spectrum of the 11Al catalysts, together with the Au foil and the unsupported Au₁₁ nanocluster as references. The pretreated catalysts before reaction were not measured due to time reasons.

In the case of the 25HT catalysts, the XANES spectra of which are displayed in Figure 4.8, the situation is different, especially in regard to the feature at 11 945 eV. When looking at the white line at 11 924 eV, the same behaviour as with the 11Mg catalysts can be observed. It can furthermore also be seen that the difference between the pure cluster and the Au foil is, in this case, smaller. This can be attributed to the different core structure of the Au₂₅ nanocluster, as compared to the Au₁₁, which could cause different electronic structures. Nevertheless, also here, all measured catalyst seem to behave as something in between the pure cluster and the Au foil. Moreover, when looking at the feature at 11 945 eV, it can be seen that the spectra of the catalysts follow the spectrum of the Au foil exactly, indicating an increase in the metallic character of the clusters.

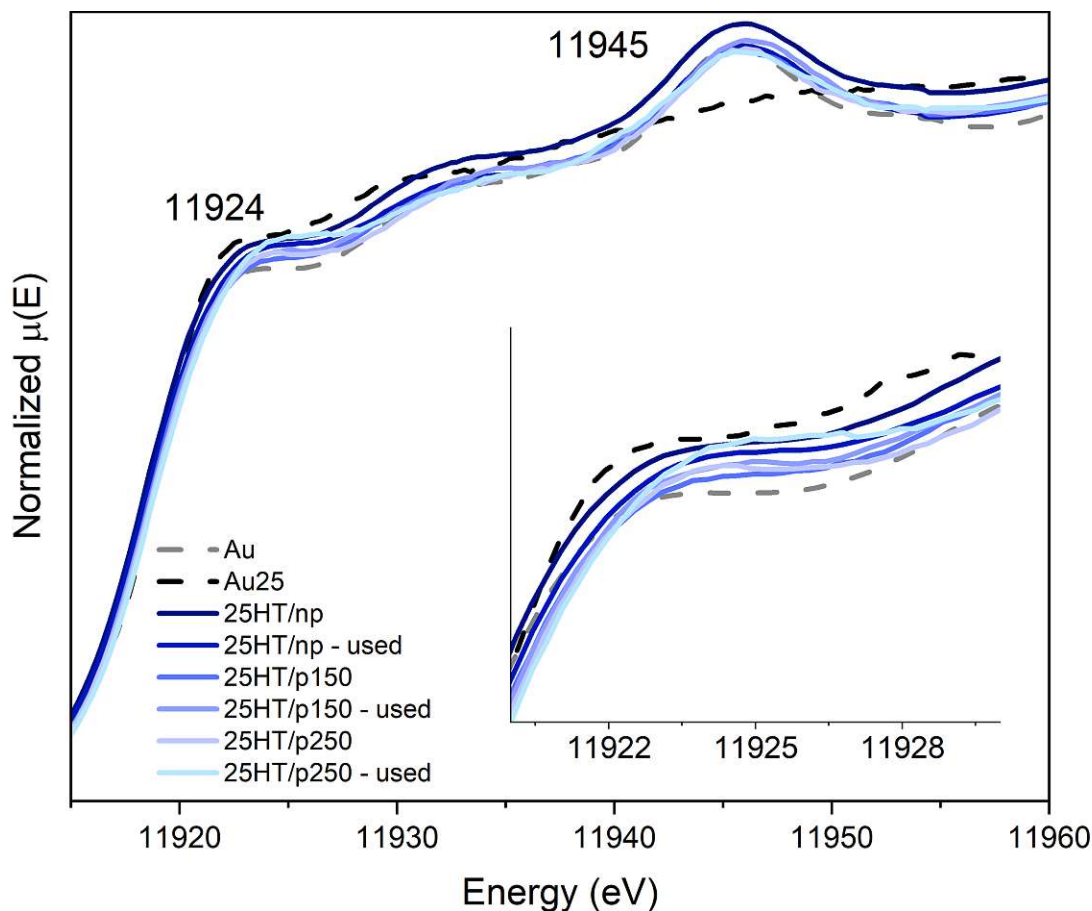


Figure 4.8.: XANES region of the XAFS spectrum of the 25HT catalysts, together with the Au foil and the unsupported Au₂₅ nanocluster as references.

Regarding the 25Mg and 25Al catalysts, due to their low levels of catalytic activity, it was expected that their XANES spectra show their instability. These are displayed in Figure 4.9 and 4.10. In the case of the 25Mg catalysts, it can be seen that after being used, they completely oxidise, as indicated by the very strong increase in the intensity of the white line. However, before the reaction, it seems that the electronic structure is mainly maintained. Nevertheless, with increasing pretreatment temperature, the white line decreases in intensity and the 25Mg/p250 sample then looks almost identical to the gold foil. Furthermore, looking at the XANES of the 25Al catalysts, it can be seen that already upon supporting, the cluster loses its electronic properties, showing that, as was the case with the Au₁₁ nanocluster, Al₂O₃ is not suitable for supporting gold nanoclusters. In both cases, the instability of the clusters can be correlated to the low levels of activity.

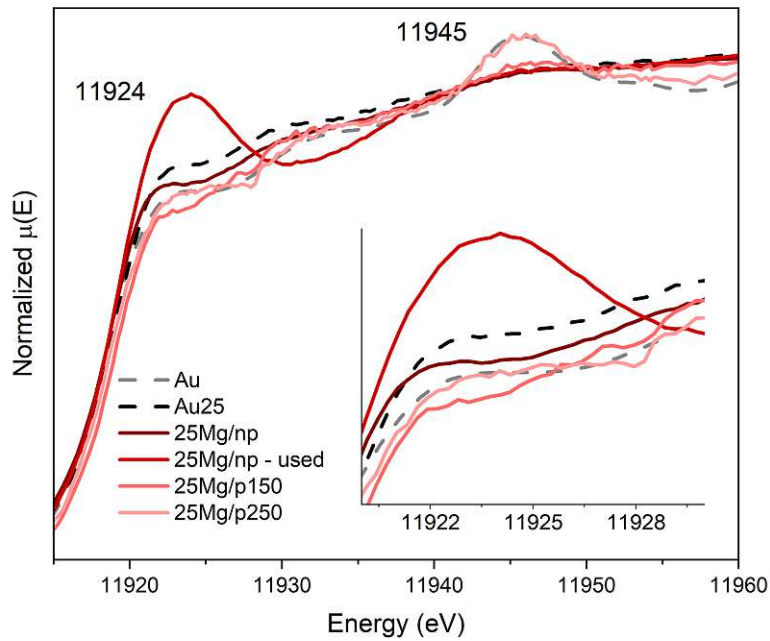


Figure 4.9.: XANES region of the XAFS spectrum of the 25Mg catalysts, together with the Au foil and the unsupported Au₂₅ nanocluster as references. Missing catalysts were not measured due to time reasons.

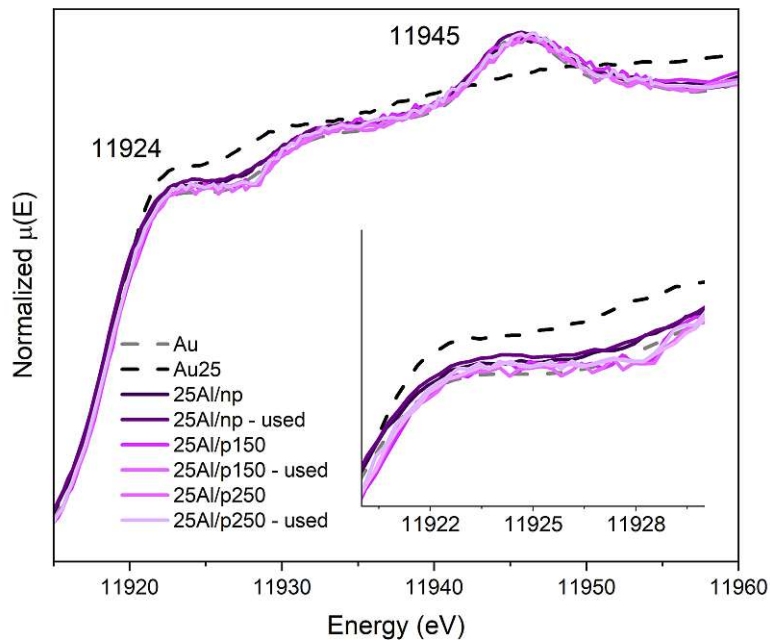


Figure 4.10.: XANES region of the XAFS spectrum of the 25Al catalysts, together with the Au foil and the unsupported Au₂₅ nanocluster as references.

EXAFS Analysis

In order to better understand the behaviour of the two catalysts that performed best, namely the 11Mg and 25HT, an in-depth EXAFS analysis was performed. The details regarding the fitting can be found in the Experimental Section. In Table 4.3, the fitted coordination numbers and radial distances for the 11Mg catalysts are shown.

Table 4.3.: Fitted coordination numbers (CN) and radial distances (R) of the 11Mg catalysts.

Sample		Au-P		Au-Au	
		R (Å)	CN	R (Å)	CN
Au11 cluster		2.32 ± 0.12	0.75 ± 0.90	2.84 ± 0.26	0.59 ± 1.10
Au11 MgO	Fresh	2.33 ± 0.06	1.80 ± 0.80	2.85 ± 0.09	0.79 ± 0.70
	Used	2.32 ± 0.06	1.26 ± 0.46	2.85 ± 0.02	2.82 ± 0.67
	Pret150	2.34 ± 0.07	1.60 ± 1.04	2.79 ± 0.13	0.63 ± 0.59
	Pret150_used	2.32 ± 0.08	1.05 ± 0.76	2.84 ± 0.03	2.62 ± 1.04
	Pret250	2.33 ± 0.07	0.94 ± 0.52	2.84 ± 0.03	2.05 ± 0.70
	Pret250_used	2.33 ± 0.11	0.92 ± 1.03	2.84 ± 0.03	3.15 ± 1.05
Au foil		/	/	2.86 ± 0.00	12 ± 0.00

On the right hand side of the table, the relations between two gold atoms are shown. As it can be seen, the distance between the gold atoms does not change, regardless of pretreatment temperature, or subjection to reaction, indicating that the structure of the core is maintained. When looking on the left side of the table, which depicts the relations between phosphorous and gold, a trend can be observed in the evolution of the CN. A slight decrease is seen both after usage of the catalyst, as well as after the pretreatment, indicating a partial loss of ligands. This is further confirmed by a slight increase of the Au-Au CN. Lastly, the stability of the Au-P distance shows that the conformation of the ligands on the core remains the same. These results confirm the hypothesis made to explain the catalytic activity, by showing that through the loss of ligands, more active sites are exposed for the hydrogen to adsorb to. Furthermore, it can also be seen that the biggest change in the CN of the Au-P happens after the pretreatment at 250 °C, confirming the supposed structural change, that lead to thee drastic change in conversion.

A more visual way to portray these results is by plotting the R-space of the EXAFS. This is depicted in Figure 4.11. Here, the change between the different catalysts becomes more visible. It can be seen that the 11Mg/np and 11Mg/p150 samples still retain some Au-P connections, whereas the other samples all lack the corresponding peak, showing the loss of ligands. What can also be seen is the similarity of some spectra with the reference measurement of the Au foil. While the fitted data does not necessarily show any particle growth, the measured spectra of especially the used catalysts show prominent features at slightly above 2 Å, which are very similar to the Au foil, which could indicate particle growth.

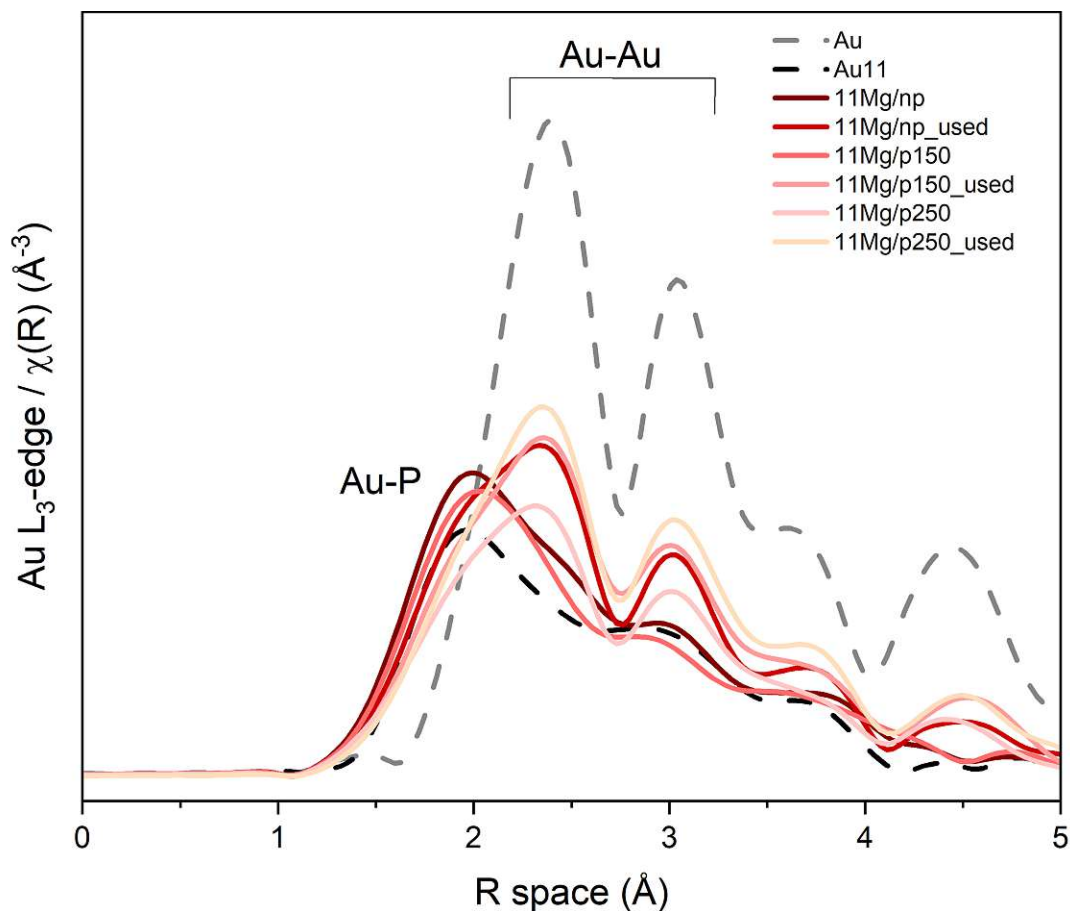


Figure 4.11.: Radial space of the EXAFS spectrum of the 11Mg catalysts, with the unsupported cluster and metallic gold foil as a reference.

Table 4.4.: Fitted coordination numbers (CN) and radial distances (R) of the 25HT catalysts.

Sample		Au-S		Au-Au	
		R (Å)	CN	R (Å)	CN
Au25 cluster		2.65 ± 0.18	1.55 ± 0.40	2.64 ± 0.14	0.48 ± 1.05
Au25 HT	Fresh	2.38 ± 0.02	1.16 ± 0.49	2.86 ± 0.02	7.98 ± 1.18
	Used	/	0.00 ± 0.79	2.85 ± 0.04	11.59 ± 1.75
	Pret150	2.42 ± 0.01	0.02 ± 0.28	2.85 ± 0.03	7.35 ± 1.18
	Pret150_used	/	0.00 ± 0.54	2.85 ± 0.06	7.51 ± 1.23
	Pret250	2.40 ± 0.07	0.52 ± 0.28	2.86 ± 0.17	7.65 ± 1.08
	Pret250_used	2.28 ± 0.05	0.18 ± 0.67	2.87 ± 0.06	8.27 ± 1.63
Au foil		/	/	2.86 ± 0.00	12 ± 0.00

For the 25HT catalyst, a similar analysis has been made, with the results being displayed

in Table 4.4. As was the case with the 11Mg catalysts, the radial distance between gold atoms in the 25HT catalysts also stayed the same throughout all samples, indicating the stability of the core. What is however even more visible in these samples, is the change in coordination number of sulphur atoms to gold. It can be seen that only the unused, unpretreated catalyst still retains some ligand connections, showing that the core is open for other molecules to adsorb to it. Furthermore, the higher Au-Au CN compared to the 11Mg catalysts indicates the bigger size of the core. The used, unpretreated sample with a slightly elevated CN as compared to the others can likely be explained by poor quality of data, considering also the large error of the calculation.

In order to better visualize the data, the R space has again been plotted and can be seen in Figure 4.12. For the fresh, unpretreated sample, a small shoulder can be seen corresponding to the gold sulphur bond, indicating the presence of ligands before the usage of the catalyst. When comparing these results with the S-K edge XANES measurements, where clear S-O features were visible, it becomes plausible that these were not caused solely by the interaction of the staples with the support, but also from ligands that got stripped away from the cluster. Furthermore, what is very visible in all spectra is the similarity to the Au foil. While the fitted data does not show particle growth, with the exception of the pore outlier, in the R space of the measured spectra it becomes visible that the sample is closer to the metallic gold foil, which corroborates that XANES results, where the feature at 11 945 eV followed the same pattern as the Au foil.

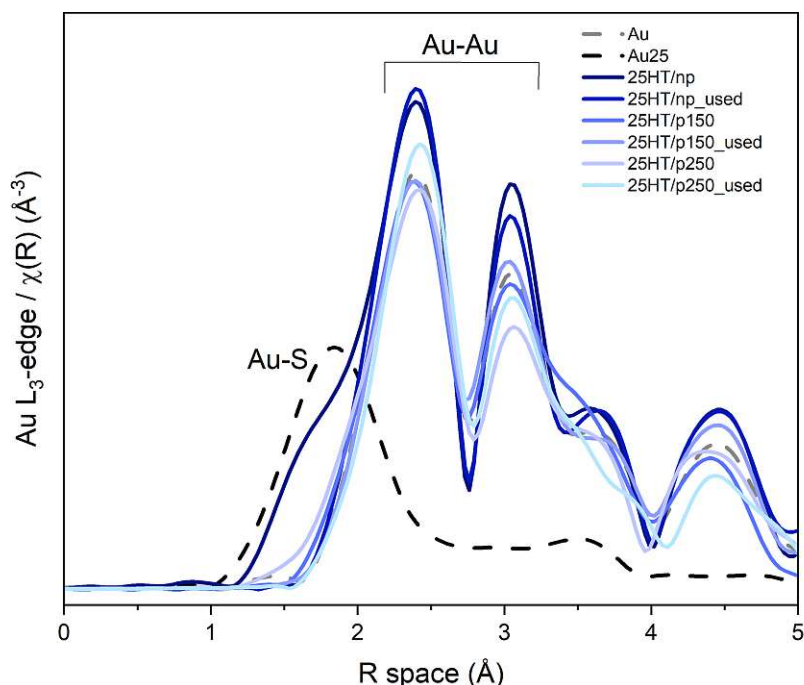


Figure 4.12.: Radial space of the EXAFS spectrum of the 25HT catalysts, with the unsupported cluster and metallic gold foil as a reference.

Considering the findings of the catalytic tests and the XAFS analysis, it can be said that there are clear correlations between the support, pretreatment and the activity of the nanoclusters in the heterogeneous semihydrogenation of alkynes. It was found that for the Au₁₁ nanoclusters, the MgO was the best support and the pretreatment had a positive effect on the catalytic activity. On the other hand, for the Au₂₅ nanoclusters, the HT supported catalysts showed the best activity. Moreover, in contrast to the 11Mg catalysts, in this case the pretreatment had a negative effect on the catalysis. Furthermore, the XAFS analysis showed the dynamic structure of the nanoclusters during the reaction, bringing to light the way the ligands are being stripped and possible particle growth phenomena.

4.2. Homogeneous Hydrogenation of Ketones

Taking the results of the tests performed in the heterogeneous system into account, it was plausible to investigate the activity of these structures also in homogeneous conditions, in order to better gauge the influence of the structure of the nanoclusters on the catalytic activity. For this purpose, two new clusters were introduced in addition to the Au₂₅(2-PET)₁₈, the Au₃₈(2-PET)₂₄ and the Au₁₄₄(2-PET)₆₀. Together with the Au₂₅ nanocluster, they were tested in the hydrogenation of ketones to alcohols. The details of the reaction procedure can be found in the Experimental Section. As previously mentioned, the core of these structures are stabilized by so-called staple units. The reason why these three nanoclusters were chosen is the different structure and arrangement of their staples, namely that the Au₂₅ has only long staples, the Au₁₄₄ only short ones and the Au₃₈ both short and long staples. The structures of the Au₃₈ and Au₁₄₄ can be seen in Figure 4.13. This particular part of the nanocluster structure has not previously been much considered when investigating the catalytic activity of nanoclusters, making it an interesting possibility. Furthermore, the Au₂₅ nanocluster was also synthesized in another ligand, the 2-MBT, in order to examine the effect of the ligand. For the Au₃ and Au₁₄₄ nanoclusters, the temperature dependence of the activity was also explored, by performing the reaction at 25, 40 and 80 °C.

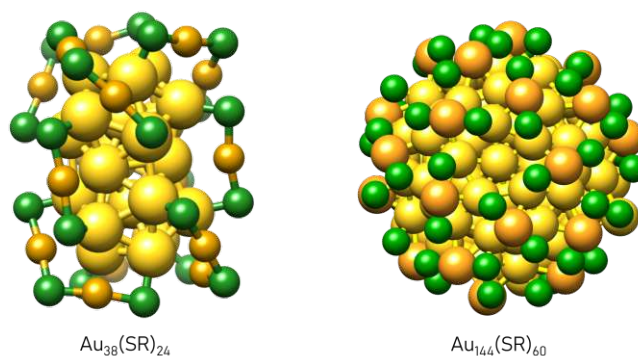


Figure 4.13.: Structures of the Au₃₈ and Au₁₄₄ nanoclusters, depicting the different staple configurations.

Compared to the heterogeneous system, the analysis of these reactions proved more problematic. Due to both the reactants and the catalyst being in the same phase. Firstly, an analysis by GC was attempted. However, to this end, the catalyst had to be separated from the reaction mixture, in order to not damage the chromatography column. To this end, several techniques were probed. To begin with, precipitation by an anti-solvent, such as hexane was tried, however, not all of the cluster could be separated. Next, evaporation of solvent was attempted, though because of the vastly smaller volume of reactant employed, this method was soon discarded, due to the possibility of reactant evaporation. Continuing, separation by silica liquid phase chromatography was tried, but also here, the clusters could not be separated quantitatively. Next a separation by size exclusion chromatography was attempted. This technique seemed to be the most promising, as the cluster could be fully separated and collected, but it did not produce reproducible results. Most likely, the reason for this is the longitudinal diffusion of the reactants inside the column. Apart from this, the sample is also strongly diluted, leading to detection difficulties of the already small amounts, as well as making quantification impossible. Finally this method was discarded as well. Lastly, the aim to separate the catalyst was dropped and the whole reaction mixture as analysed by HPLC. While this technique is rather time consuming, due to the long method times, it proved to be the most facile. The calibration performed can be found in the Experimental Section. The results of the catalytic tests are discussed in the following.

4.2.1. Catalytic Activity in Homogeneous Phase

The catalytic activity of the nanoclusters, measured by HPLC, is displayed in Table 4.5. The first thing to note is the difference in conversion between the Au₂₅ catalyst with the 2-MBT and 2-PET ligands. Because the 2-MBT is less bulky compared to the 2-PET, it would be expected that the cluster with the 2-MBT is more active, since the core of the cluster is more accessible for the hydrogen. However, the opposite seems to be the case, indicating a strong effect of the ligand on the catalytic activity, especially considering the structural similarity of the substrate acetophenone to the 2-PET. Furthermore, the temperature dependence of the Au₃₈ and Au₁₄₄ shows an interesting behaviour. While for the Au₃₈ an increase of temperature influences the catalytic activity negatively, the opposite is true for the Au₁₄₄. This could be related to their different staple configurations. Looking at their structures, which are presented in Figure 4.13, it can be seen that due to the long staple units of the Au₃₈, the Au core is rather accessible for molecules to adsorb to it. On the other hand however, the core of the Au₁₄₄ is solely protected by short staples which cover most of the core atoms. Considering the effect found in the heterogeneous system, that at elevated temperature the staple units are stripped from the cluster, it is plausible to assume a similar process also in the homogeneous system. Moreover, keeping in mind that because the clusters are not immobilized on a surface their structure is even more dynamic, it would also be expected that this barrier is much lower.

Table 4.5.: Catalytic results of the clusters in homogeneous system, with different ligands and at different temperatures.

Cluster	Ligand	T (°C)	Conversion (%)
Au25	2-MBT	25	56
	2-PET	25	>99
Au38	2-PET	25	>99
		40	65
		80	54
Au144	2-PET	25	67
		40	66
		80	>99

In the following image (Figure 4.14, excerpts of the chromatograms are shown). It can be seen that the product distribution is slightly different for each catalyst. Interestingly, although the precursor peak was at times no longer visible, no product peaks could be observed. This likely indicates a too strong reaction and either a complete degradation of the desired product, or the continuing reaction of the desired product to other compounds, such as fully reduced alkanes. In order to improve this, it is necessary to tune the reaction conditions further, by perhaps shortening the reaction time, or reducing the hydrogen pressure. It seems that at least for the Au₁₄₄, a certain temperature is necessary to activate the cluster, so varying this parameter will likely not make a strong difference anymore. Apart from tuning the reaction parameters, a more robust analysis method must also be looked into.

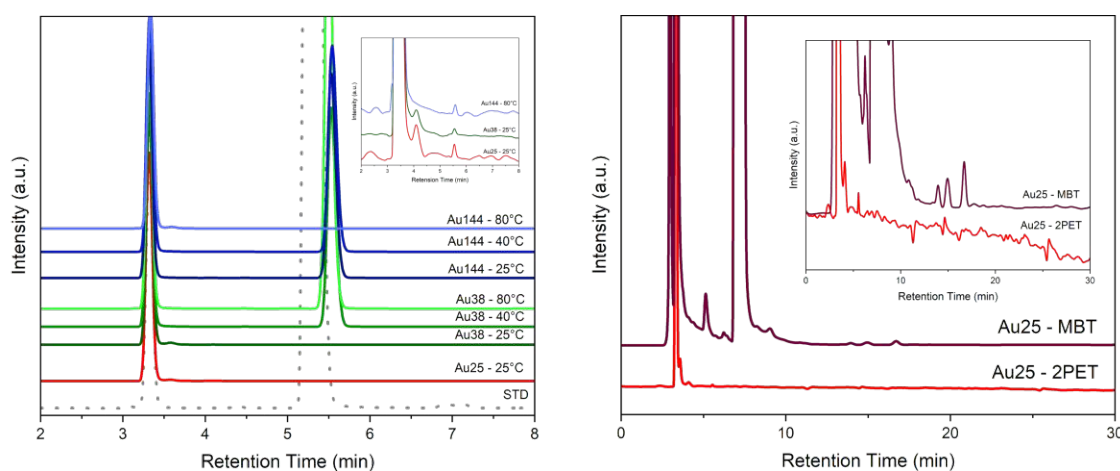


Figure 4.14.: HPLC chromatograms of the reaction mixture, after the reaction was performed with the different catalysts, as well as a standard (STD) containing all reactants and solvents. The peak around 3.25 min corresponds to a mixture of toluene and the catalyst and the one at around 5.5 min to acetophenone.

Continuing, another aspect that needed to be considered was the stability of the clusters in the reaction solution. For this purpose UV-Vis and MALDI-MS spectra were taken before and after the reaction of each catalyst and compared to literature^[46, 48, 56]. For the Au₃₈ nanocluster, no UV-Vis could be taken, due to the small amount of sample. The spectra are displayed in the following Figure 4.15. It can be seen that the bands corresponding to the specific clusters are retained after the reaction, with negligible deviations. Therefore, it can be said that even without a support, gold nanoclusters are stable under reaction conditions. The spectra are taken of the samples that showed the best activity, namely the Au₂₅(2-PET)₁₈, the Au₃₈ at 25 °C and the Au₁₄₄ at 80 °C.

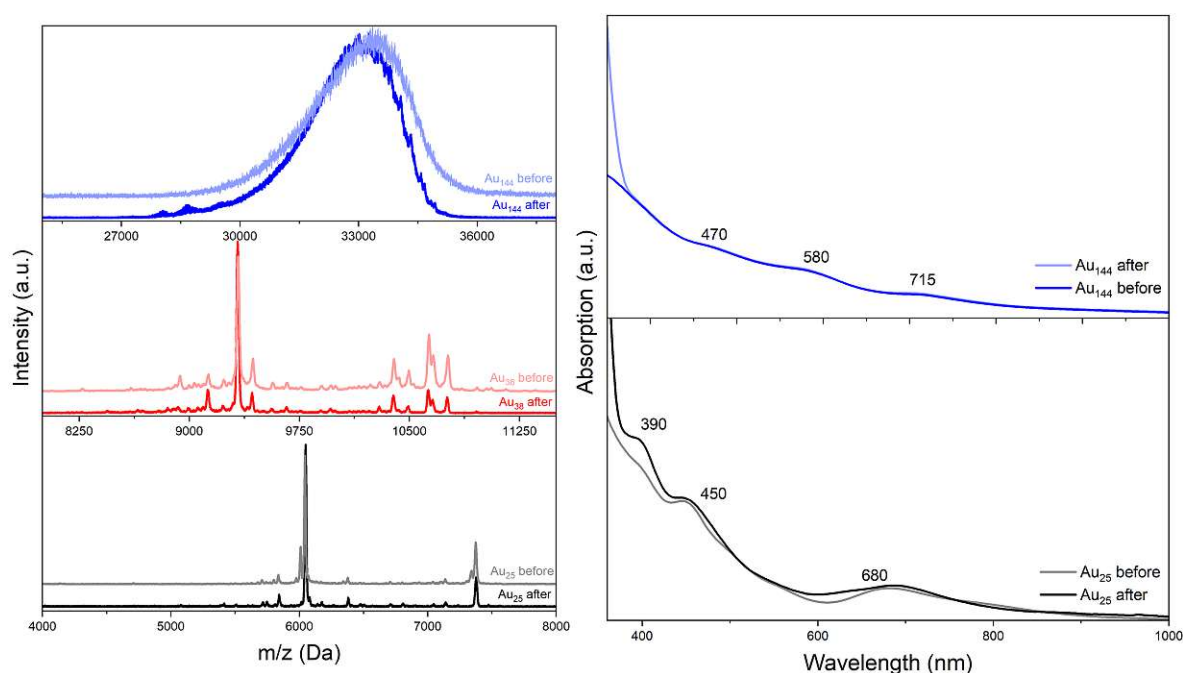


Figure 4.15.: Left panel: MALDI-MS spectra of the nanoclusters before and after the reaction. Right panel: UV-Vis spectra of the cluster before and after the reaction (Au₃₈ missing due to too small amount of sample for accurate measurement)

While these results look very promising, it has to be said that a more in-depth analysis of this system is necessary, in order to draw any definite conclusions. To begin with, the use of the coupling of HPLC with mass spectrometry would shed a lot more light on the outcome of the reaction, as a definite characterization of each peak would be possible. Barring this, a NMR analysis of could help shed some light on the nature of the products. Continuing, a fine tuning of the reaction parameters is needed, in order to steer the reaction towards the desired outcome. Nevertheless, it can be said that the staples of these structures, as well as the ligand, perhaps even the similarity of the ligand to the substrate, all have an influence on the catalytic process.

5. Conclusions and Outlook

Summarizing, gold nanoclusters have been tested as both heterogeneous and homogeneous catalysts in the semihydrogenation of alkynes and the reduction of ketones, respectively. For heterogeneous catalysis, two different clusters with different ligands were synthesized, namely the $\text{Au}_{11}(\text{PPh}_3)_7\text{Br}_3$ and the $\text{Au}_{25}(2\text{-PET})_{18}$. They were both supported on three different metal oxides, MgO, Al_2O_3 and HT, chosen for their different basicity. Each catalyst was then pretreated at two different temperatures. Through this, the effect of the ligands, pretreatment and support could be investigated.

The first observation made was that there seems to be clear correlations between the cluster-support interaction and the catalytic activity. In the case of the Au_{11} catalysts, only the ones supported on MgO performed satisfactorily, showing almost 100 % conversion and very high selectivity towards styrene, whereby the pretreatment had a positive effect on the conversion rate. This was explained on the one hand by the basicity of the MgO, which was reported to favour the cleavage of the H_2 bond. The increase in activity after pretreating at 250 °C was hypothesized to be due to a change in the structure of the nanocluster. XAFS analysis revealed that by pretreating at higher temperatures, ligands are cleaved from the core, thereby exposing more active sites where the hydrogen could adsorb and be activated. In the case of the Au_{25} catalysts however, the ones supported on HT performed best, with a conversion of around 75 % and a selectivity of about 15 %. Here however, the pretreatment had a negative effect. This could be explained by the different structures of the clusters. While in the case of the Au_{11} the ligands are directly connected to the core, in the case of thiolate protected nanoclusters, staple formations are found, which shelter the core. When pretreating at higher temperatures, these staple formations are removed from the cluster, thereby opening the core. Because of the different size and therefore electronic structure of the core, it appears that phenylacetylene could bind to the metal as a ligand, thereby poisoning the catalyst. The XAFS analysis of these catalysts showed that even without pretreatment, most, if not all of the ligands are lost after performing the reaction. Furthermore, regarding the lower selectivity of the thiolate protected nanocluster catalysts, experiments were done in order to gauge the nature of the other products formed. It was found that by running the reaction with only the ligand, some of the precursor phenylacetylene was used, however no product was formed, indicating that the ligand itself reacted with the alkyne to form other compounds. Considering the observed loss of ligands, it is plausible to assume that the free ligand cleaved from the cluster underwent a reaction with the phenylacetylene.

Regarding the XAFS analysis, the XANES region showed that none of the catalysts

followed the electronic structure of neither the pure cluster, nor of metallic gold. Therefore, it should be assumed that there is some interaction between the clusters and their support leading in a change of electronic structure. Moreover, it was visible that in the case of the 11Mg catalysts, all samples showed more or less the same spectrum, which speaks for their stability. On the other hand, both the 11Al and 11HT catalysts showed clear changes in their XANES spectra, indicating significant changes in their electronic structure, which could be interpreted as oxidation or particle growth. In the case of the Au₂₅ catalysts it could be seen that the spectra all followed the same trend in the case of the 25HT. However, in contrast to 11Mg, these catalysts showed a strong resemblance to the gold foil in the feature at 11 945 eV, indicating structural changes. The other catalysts proved to be unstable, due to strong changes visible in the spectra. When analysing the EXAFS region, the indications of the XANES analysis and the assumptions from the catalytic activity tests could be explained. In the case of the 11Mg catalysts, it became clearly visible how the ligands are cleaved, through the decreasing coordination number Au-P. However, the stable CN Au-Au and the remaining radial distance indicate that nor particle growth is present. For the 25HT catalysts, the loss of ligands becomes clearly visible, through the strong decline of the Au-S CN, especially in the samples measured after the reaction. When looking at the plotted radial space, stark similarities with the gold foil can be seen, which can explain the behaviour of the feature at 11 945 eV in the XANES spectrum. This, together with the slightly increased Au-Au CN, could indicate slight particle growth, which could explain the lesser activity of the clusters. Regarding the analysis done on the S-K edge of these clusters, where strong S-O bands could be seen, it can be assumed that these largely correspond to loss of ligands.

Considering these findings, it can be concluded that the ligands, pretreatment and support of the nanocluster catalysts all have a strong effect on their catalytic activity. In order to better understand the influence of the cluster structure itself, the clusters were tested in the homogeneous reduction of acetophenone to 1-phenylethanol. For this purpose, two new clusters were synthesized, chosen for their different staple configurations, namely the Au₃₈(2-PET)₂₄ and the Au₁₄₄(2-PET)₆₀, as well as another Au₂₅ nanocluster, with 2-MBT as ligand. These preliminary results show that the different staple configurations seem to have an effect on the catalytic activity. It appears that at lower temperatures, longer staples that allow more access to the core are favoured, as they allow the hydrogen to be activated, whereas at elevated temperature, the short stapled Au₁₄₄ nanocluster performs better. This could be explained through a similar phenomenon as the one observed in the heterogeneous system, where ligands are stripped at elevated temperatures. By heating up the cluster, it appears that ligands are lost, thereby opening up the core and allowing the hydrogen to be activated.

These combined results show that it is necessary to consider the whole structure of the catalyst when designing an experiment and understand the influence of each parameter in part, in order to be able to optimize the catalyst properly.

Moving forward, it is necessary to further optimize the heterogeneous system, in order to maximise the selectivity, especially in the case of the 25Mg catalysts. Furthermore, in order to make these catalysts more attractive to industry, they should be tried with a real-life feed, in gas phase. Regarding the use of gold nanoclusters as homogeneous catalysts, it can be concluded that these results present important information about the influence the different parts of the clusters have on the catalysis and how they interact with the substrate. However, while these preliminary results are promising, it is important to complete the work by optimizing the reaction parameters and especially the analysis method. Ideally, a coupling of HPLC with MS should be used, in order to identify all reaction compounds with certainty. Barring this, the use of NMR spectroscopy could also give some insights. Moreover, in order to make the application of these catalysts more attractive, the reaction should be performed using chiral clusters, in order to enantioselectively synthesize the corresponding alcohols, which could then be used as precursors for drug development. Finally, moving this type of catalysis to heterogeneous system is desired, in order to facilitate analysis and reaction protocols.

In light of all aspects discussed, it can be said that gold nanoclusters proved to be potent and efficient as both homogeneous and heterogeneous catalysts in selective hydrogenation reactions. Being able to study all structural components separately was shown to be of great importance, as it gave insights on the different ways the catalysts could be improved. All things considered, this work shows that gold nanoclusters are not only a powerful system for fundamental studies, but also competitive catalysts, well worth being considered for real-life applications.

Appendix

A. Appendix

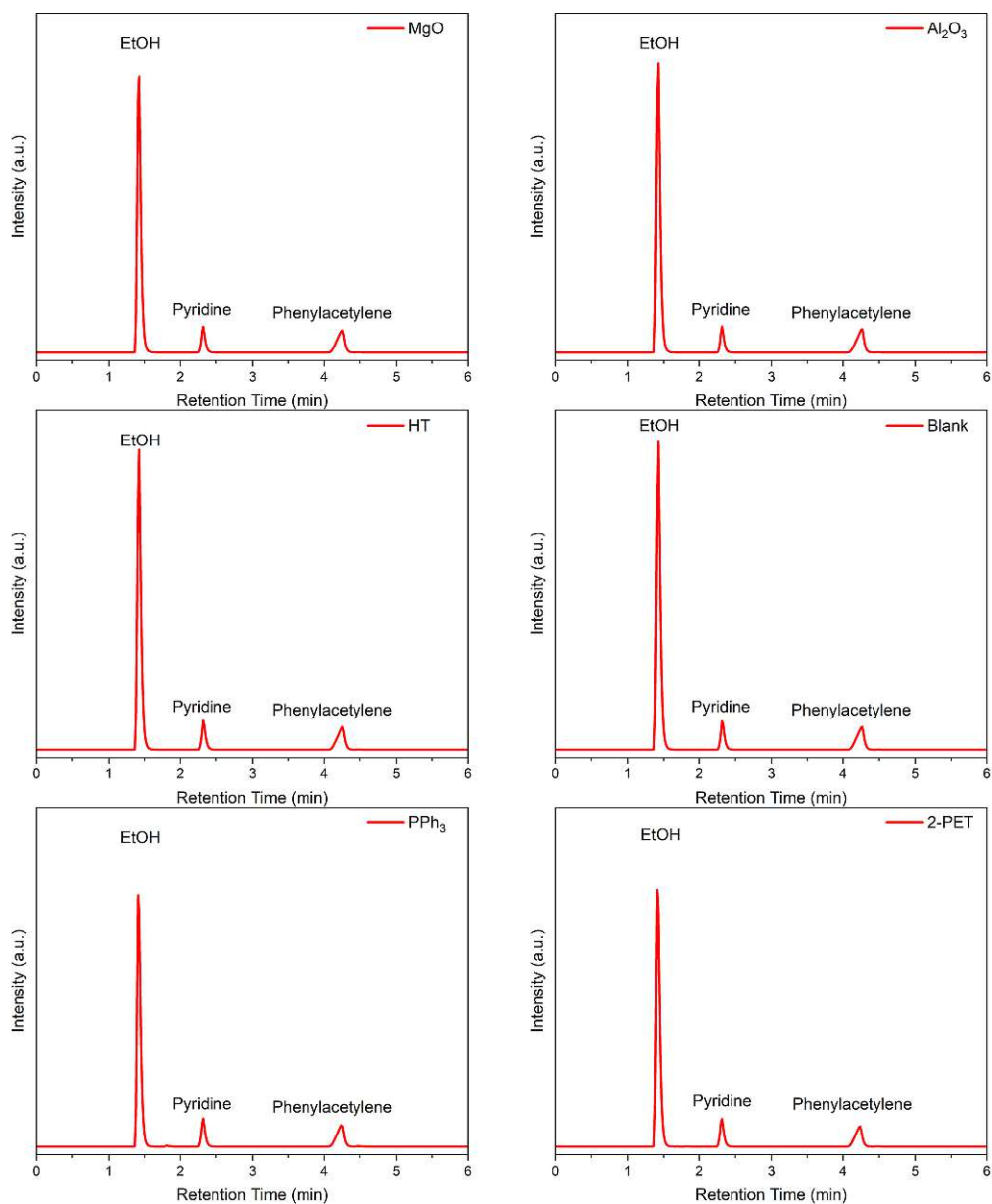


Figure A.1.: Blanks for the semihydrogenation tests.

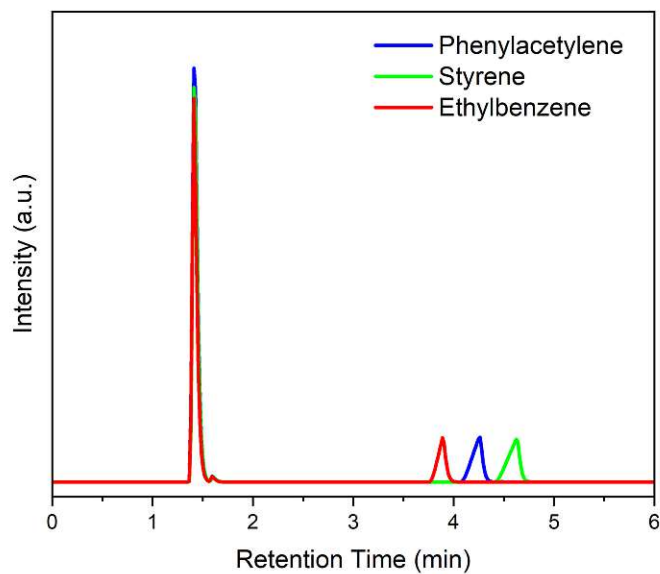


Figure A.2.: Example chromatogramm of the standards for the semihydrogenation tests.

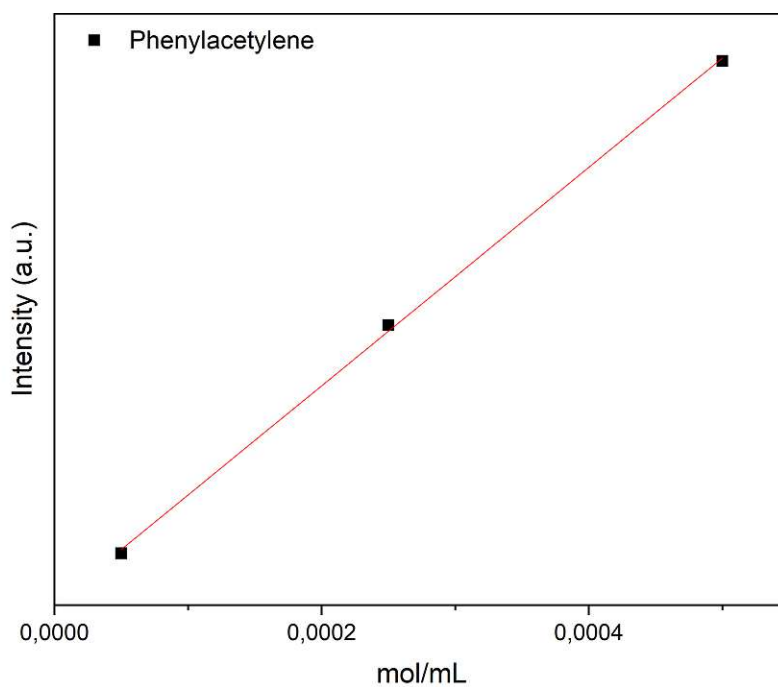


Figure A.3.: Phenylacetylene calibration

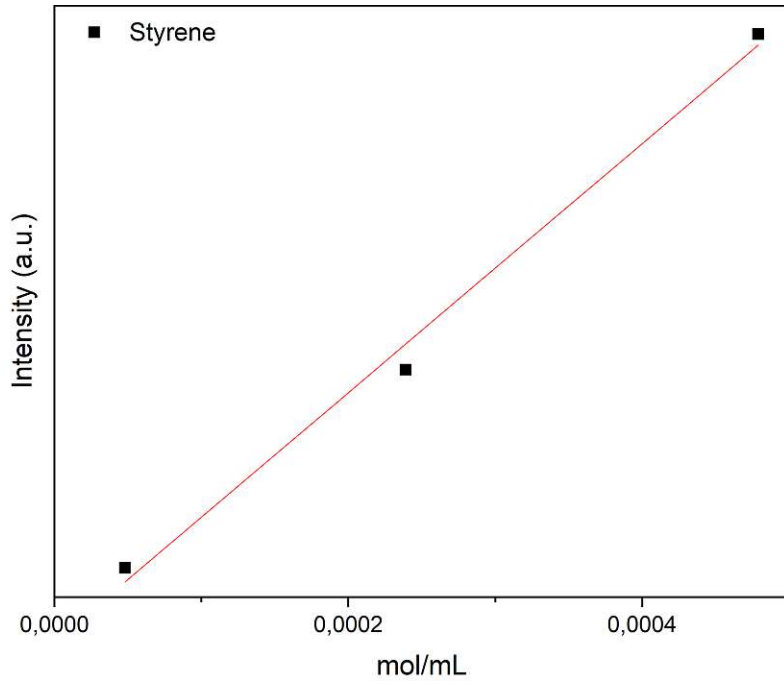


Figure A.4.: Styrene calibration

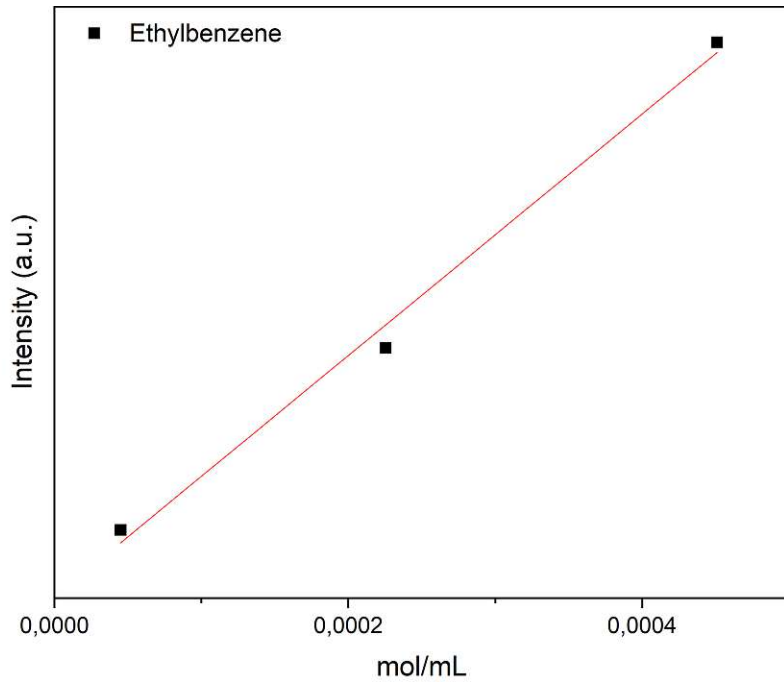


Figure A.5.: Ethylbenzene calibration

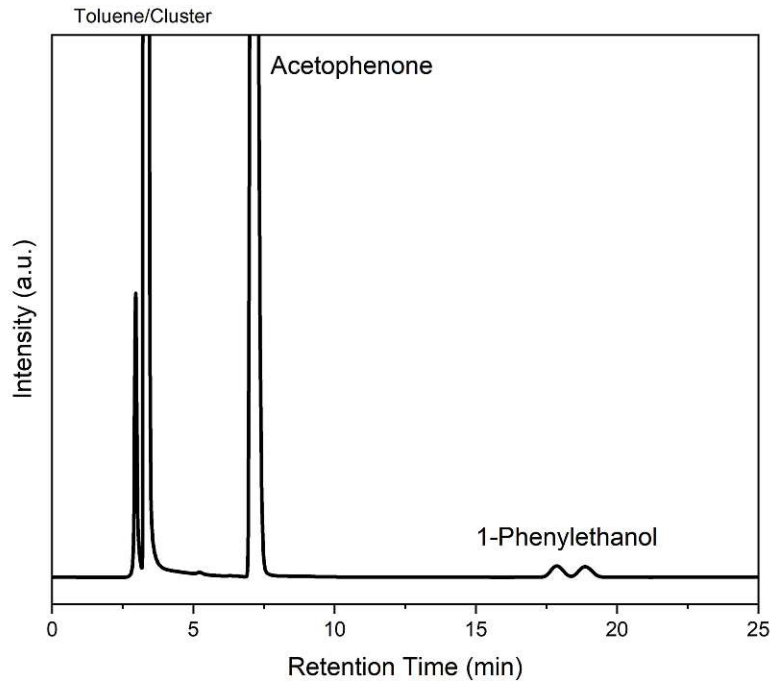


Figure A.6.: Acetophenone reduction standards

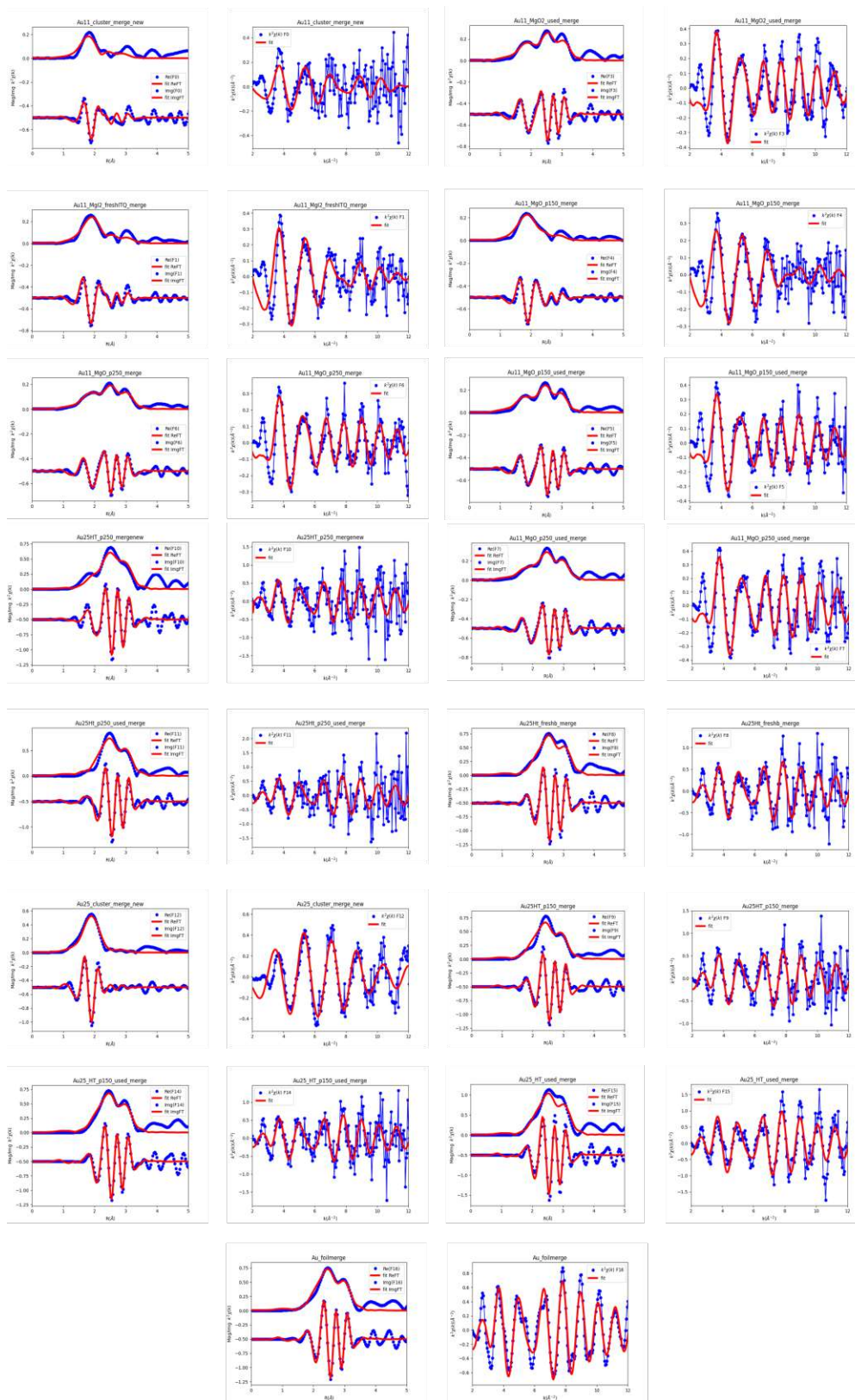


Figure A.7.: EXAFS fitting

List of Figures

1.1. Example of the size-focusing synthesis method for thiolate protected gold nanoclusters.	3
1.2. Detailed structure of two prevalent nanoclusters, exemplifying the similarities and differences between thiolate and phosphine protected nanoclusters.	5
1.3. Reaction pathway of the reduction of phenylacetylene (blue) to styrene (green; the desired product) and finally to ethylbenzene (red; undesired product).	6
1.4. Scheme of supported nanoclusters.	9
1.5. Scheme of the reaction investigated in homogeneous catalysis.	9
3.1. UV-Vis spectrum of the pure $\text{Au}_{11}(\text{PPh}_3)_7\text{Br}_3$ nanocluster.	13
4.1. Structure of the synthesized nanoclusters.	20
4.2. Conversion of phenylacetylene is represented by the total height of the bar. The different colors represent the selectivity of the Au_{11} catalysts toward styrene (ST), ethylbenzene (EB) and other side-products (Other). The level of pretreatment is indicated by the abbreviations next to the catalyst name, with <i>np</i> meaning no pretreatment, <i>p150</i> referring to pretreatment at 150 °C and <i>p250</i> at 250 °C.	21
4.3. Conversion of phenylacetylene is represented by the total height of the bar. The different colors represent the selectivity of the Au_{25} catalysts toward styrene (ST), ethylbenzene (EB) and other side-products (Other). The level of pretreatment is indicated by the abbreviations next to the catalyst name, with <i>np</i> meaning no pretreatment, <i>p150</i> referring to pretreatment at 150 °C and <i>p250</i> at 250 °C.	23
4.4. XRD measurement of the 11Mg and 25HT catalysts, with the bare support as reference.	25
4.5. XANES region of the XAFS spectrum of the 11Mg catalysts, together with the Au foil and the unsupported Au_{11} nanocluster as references.	26
4.6. XANES region of the XAFS spectrum of the 11HT catalysts, together with the Au foil and the unsupported Au_{11} nanocluster as references.	27
4.7. XANES region of the XAFS spectrum of the 11Al catalysts, together with the Au foil and the unsupported Au_{11} nanocluster as references. The pretreated catalysts before reaction were not measured due to time reasons.	28

4.8. XANES region of the XAFS spectrum of the 25HT catalysts, together with the Au foil and the unsupported Au ₂₅ nanocluster as references.	29
4.9. XANES region of the XAFS spectrum of the 25Mg catalysts, together with the Au foil and the unsupported Au ₂₅ nanocluster as references. Missing catalysts were not measured due to time reasons.	30
4.10. XANES region of the XAFS spectrum of the 25Al catalysts, together with the Au foil and the unsupported Au ₂₅ nanocluster as references.	30
4.11. Radial space of the EXAFS spectrum of the 11Mg catalysts, with the unsupported cluster and metallic gold foil as a reference.	32
4.12. Radial space of the EXAFS spectrum of the 25HT catalysts, with the unsupported cluster and metallic gold foil as a reference.	33
4.13. Structures of the Au ₃₈ and Au ₁₄₄ nanoclusters, depicting the different staple configurations.	34
4.14. HPLC chromatograms of the reaction mixture, after the reaction was performed with the different catalysts, as well as a standard (STD) containing all reactants and solvents. The peak around 3.25 min corresponds to a mixture of toluene and the catalyst and the one at around 5.5 min to acetophenone. . . .	36
4.15. Left panel: MALDI-MS spectra of the nanoclusters before and after the reaction. Right panel: UV-Vis spectra of the cluster before and after the reaction (Au ₃₈ missing due to too small amount of sample for accurate measurement)	37
A.1. Blanks for the semihydrogenation tests.	42
A.2. Example chromatogramm of the standards for the semihydrogenation tests. .	43
A.3. Phenylacetylene calibration	43
A.4. Styrene calibration	44
A.5. Ethylbenzene calibration	44
A.6. Acetophenone reduction standards	45
A.7. EXAFS fitting	46

List of Tables

3.1. Fitting parameters for the EXAFS spectra.	18
4.1. Yield towards styrene of the Au ₁₁ catalysts.	22
4.2. Yield towards styrene of the Au ₂₅ catalysts.	24
4.3. Fitted coordination numbers (CN) and radial distances (R) of the 11Mg catalysts. 31	
4.4. Fitted coordination numbers (CN) and radial distances (R) of the 25HT catalysts. 32	
4.5. Catalytic results of the clusters in homogeneous system, with different ligands and at different temperatures.	36

Bibliography

- [1] Maximilian L. Spiekermann and Thomas Seidensticker. Catalytic processes for the selective hydrogenation of fats and oils: reevaluating a mature technology for feedstock diversification. *Catalysis Science and Technology*, 2024.
- [2] I. S. Chemakina, M. I. Ivantsov, M. V. Kulikova, N. Yu. Tretyakov, and A. V. Elyshev. Carbon-based catalysts for selective hydrogenation of carbon oxides (methanation). *Petroleum Chemistry*, 63(6):693–697, June 2023.
- [3] David Decker, Hans-Joachim Drexler, Detlef Heller, and Torsten Beweries. Homogeneous catalytic transfer semihydrogenation of alkynes: an overview of hydrogen sources, catalysts and reaction mechanisms. *Catalysis Science and Technology*, 10(19):6449–6463, 2020.
- [4] Piet W. N. M. van Leeuwen. *Recent Advances in Nanoparticle Catalysis*. Number v.1 in Molecular Catalysis Ser. Springer International Publishing AG, Cham, 2020. Description based on publisher supplied metadata and other sources.
- [5] Jordan Santiago Martinez, Jaime Mazarío, Christian Wittee Lopes, Susana Trasobares, José Juan Calvino Gamez, Giovanni Agostini, and Pascual Ona-Burgos. Efficient alkyne semihydrogenation catalysis enabled by synergistic chemical and thermal modifications of a pdin mof. *ACS Catalysis*, 14(7):4768–4785, March 2024.
- [6] Chenming Huang, Junling Liu, Jiali Fang, Xian Jia, Zhendong Zheng, Song You, and Bin Qin. Ketoreductase catalyzed (dynamic) kinetic resolution for biomanufacturing of chiral chemicals. *Frontiers in Bioengineering and Biotechnology*, 10, June 2022.
- [7] Yasuhiro Kawanami and Ryo C. Yanagita. Practical enantioselective reduction of ketones using oxazaborolidine catalysts generated in situ from chiral lactam alcohols. *Molecules*, 23(10):2408, September 2018.
- [8] Afifa Ayu Koesoema, Daron M. Standley, Toshiya Senda, and Tomoko Matsuda. Impact and relevance of alcohol dehydrogenase enantioselectivities on biotechnological applications. *Applied Microbiology and Biotechnology*, 104(7):2897–2909, February 2020.
- [9] Jorge A. Delgado, Olivia Benkirane, Carmen Claver, Daniel Curulla-Ferré, and Cyril Godard. Advances in the preparation of highly selective nanocatalysts for the semihydrogenation of alkynes using colloidal approaches. *Dalton Transactions*, 46(37):12381–12403, 2017.

- [10] Blaise Bridier, Núria López, and Javier Pérez-Ramírez. Molecular understanding of alkyne hydrogenation for the design of selective catalysts. *Dalton Transactions*, 39(36):8412, 2010.
- [11] Zhe Wang, Qian Luo, Shanjun Mao, Chunpeng Wang, Jinqi Xiong, Zhirong Chen, and Yong Wang. Fundamental aspects of alkyne semi-hydrogenation over heterogeneous catalysts. *Nano Research*, 15(12):10044–10062, July 2022.
- [12] Davide Albani, Masoud Shahrokhi, Zupeng Chen, Sharon Mitchell, Roland Hauert, Núria López, and Javier Pérez-Ramírez. Selective ensembles in supported palladium sulfide nanoparticles for alkyne semi-hydrogenation. *Nature Communications*, 9(1), July 2018.
- [13] Shanjun Mao, Bowen Zhao, Zhe Wang, Yutong Gong, Guofeng Lü, Xiao Ma, Lili Yu, and Yong Wang. Tuning the catalytic performance for the semi-hydrogenation of alkynols by selectively poisoning the active sites of pd catalysts. *Green Chemistry*, 21(15):4143–4151, 2019.
- [14] Jianbo Zhao, Liming Ge, Haifeng Yuan, Yingfan Liu, Yanghai Gui, Baoding Zhang, Liming Zhou, and Shaoming Fang. Heterogeneous gold catalysts for selective hydrogenation: from nanoparticles to atomically precise nanoclusters. *Nanoscale*, 11(24):11429–11436, 2019.
- [15] Nikolaos Dimitratos, Gianvito Vilé, Stefania Albonetti, Fabrizio Cavani, Jhonatan Fiorio, Núria López, Liane M. Rossi, and Robert Wojcieszak. Strategies to improve hydrogen activation on gold catalysts. *Nature Reviews Chemistry*, 8(3):195–210, February 2024.
- [16] Rongchao Jin, Chenjie Zeng, Meng Zhou, and Yuxiang Chen. Atomically precise colloidal metal nanoclusters and nanoparticles: Fundamentals and opportunities. *Chemical Reviews*, 116(18):10346–10413, September 2016.
- [17] Rohul H. Adnan, Jenica Marie L. Madridejos, Abdulrahman S. Alotabi, Gregory F. Metha, and Gunther G. Andersson. A review of state of the art in phosphine ligated gold clusters and application in catalysis. *Advanced Science*, 9(15), March 2022.
- [18] Robert L. Donkers, Dongil Lee, and Royce W. Murray. Synthesis and isolation of the molecule-like cluster $\text{Au}_{38}(\text{phch}_2\text{ch}_2\text{s})_{24}$. *Langmuir*, 20(5):1945–1952, January 2004.
- [19] Yuichi Negishi, Katsuyuki Nobusada, and Tatsuya Tsukuda. Glutathione-protected gold clusters revisited: Bridging the gap between gold(i) thiolate complexes and thiolate-protected gold nanocrystals. *Journal of the American Chemical Society*, 127(14):5261–5270, March 2005.
- [20] Manzhou Zhu, Eric Lanni, Niti Garg, Mark E. Bier, and Rongchao Jin. Kinetically controlled, high-yield synthesis of Au_{25} clusters. *Journal of the American Chemical Society*, 130(4):1138–1139, January 2008.

- [21] Benjamin S. Gutrath, Ulli Englert, Yutian Wang, and Ulrich Simon. A missing link in undecagold cluster chemistry: Single crystal x-ray analysis of $[\text{Au}_{11}(\text{PPh}_3)_7\text{Cl}_3]$. *European Journal of Inorganic Chemistry*, 2013(12):2002–2006, March 2013.
- [22] Zhikun Wu and Rongchao Jin. Exclusive synthesis of $\text{Au}_{11}(\text{PPh}_3)_8\text{Br}_3$ against the cl analogue and the electronic interaction between cluster metal core and surface ligands. *Chemistry A European Journal*, 19(37):12259–12263, August 2013.
- [23] I. Vezmar, M. M. Alvarez, J. T. Khoury, B. E. Salisbury, M. N. Shafigullin, and R. L. Whetten. Cluster beams from passivated nanocrystals. *Zeitschrift für Physik D Atoms, Molecules and Clusters*, 40(1-4):147–151, May 1997.
- [24] H. Häkkinen, R. N. Barnett, and U. Landman. Electronic structure of passivated $\text{Au}_{38}(\text{SCH}_3)_{24}$ nanocrystal. *Physical Review Letters*, 82(16):3264–3267, April 1999.
- [25] I. L. Garzón, C. Rovira, K. Michaelian, M. R. Beltrán, P. Ordejón, J. Junquera, D. Sánchez-Portal, E. Artacho, and J. M. Soler. Do thiols merely passivate gold nanoclusters? *Physical Review Letters*, 85(24):5250–5251, December 2000.
- [26] Hannu Häkkinen, Michael Walter, and Henrik Grönbeck. Divide and protect: Capping gold nanoclusters with molecular gold thiolate rings. *The Journal of Physical Chemistry B*, 110(20):9927–9931, April 2006.
- [27] Hannu Häkkinen. Atomic and electronic structure of gold clusters: understanding flakes, cages and superatoms from simple concepts. *Chemical Society Reviews*, 37(9):1847, 2008.
- [28] Olga Lopez-Acevedo, Hironori Tsunoyama, Tatsuya Tsukuda, Hannu Häkkinen, and Christine M. Aikens. Chirality and electronic structure of the thiolate-protected Au_{38} nanocluster. *Journal of the American Chemical Society*, 132(23):8210–8218, May 2010.
- [29] Pablo D. Jadzinsky, Guillermo Calero, Christopher J. Ackerson, David A. Bushnell, and Roger D. Kornberg. Structure of a thiol monolayer-protected gold nanoparticle at 1.1 Å resolution. *Science*, 318(5849):430–433, October 2007.
- [30] Iur Horiuti and M. Polanyi. Exchange reactions of hydrogen on metallic catalysts. *Transactions of the Faraday Society*, 30:1164, 1934.
- [31] Masatake Haruta, Tetsuhiko Kobayashi, Hiroshi Sano, and Nobumasa Yamada. Novel gold catalysts for the oxidation of carbon monoxide at a temperature far below 0 °C. *Chemistry Letters*, 16(2):405–408, February 1987.
- [32] Ru-Yi Zhong, Ke-Qiang Sun, Yong-Chun Hong, and Bo-Qing Xu. Impacts of organic stabilizers on catalysis of Au nanoparticles from colloidal preparation. *ACS Catalysis*, 4(11):3982–3993, October 2014.

- [33] Balaram S. Takale, Xiujuan Feng, Ye Lu, Ming Bao, Tienan Jin, Taketoshi Minato, and Yoshinori Yamamoto. Unsupported nanoporous gold catalyst for chemoselective hydrogenation reactions under low pressure: Effect of residual silver on the reaction. *Journal of the American Chemical Society*, 138(32):10356–10364, August 2016.
- [34] Takato Mitsudome and Kiyotomi Kaneda. Gold nanoparticle catalysts for selective hydrogenations. *Green Chemistry*, 15(10):2636, 2013.
- [35] S. A. Nikolaev and V. V. Smirnov. Selective hydrogenation of phenylacetylene on gold nanoparticles. *Gold Bulletin*, 42(3):182–189, September 2009.
- [36] Xiao Yan Liu, Aiqin Wang, Tao Zhang, and Chung-Yuan Mou. Catalysis by gold: New insights into the support effect. *Nano Today*, 8(4):403–416, August 2013.
- [37] Hanbao Chong and Manzhou Zhu. Catalytic reduction by quasi homogeneous gold nanoclusters in the liquid phase. *ChemCatChem*, 7(15):2296–2304, July 2015.
- [38] Xian-Kai Wan, Jia-Qi Wang, Zi-Ang Nan, and Quan-Ming Wang. Ligand effects in catalysis by atomically precise gold nanoclusters. *Science Advances*, 3(10):e1701823, October 2017.
- [39] Site Li, Xiangsha Du, Zhongyu Liu, Yingwei Li, Yucai Shao, and Rongchao Jin. Size effects of atomically precise gold nanoclusters in catalysis. *Precision Chemistry*, 1(1):14–28, March 2023.
- [40] Stephan Pollitt, Vera Truttman, Thomas Haunold, Clara García, Wojciech Olszewski, Jordi Llorca, Noelia Barrabés, and Günther Rupprechter. The dynamic structure of $\text{Au}_{38}(\text{SR})_{24}$ nanoclusters supported on CeO_2 upon pretreatment and co oxidation. *ACS Catalysis*, 10(11):6144–6148, May 2020.
- [41] I. López-Hernández, V. Truttman, N. Barrabés, G. Rupprechter, F. Rey, J. Mengual, and A.E. Palomares. Gold nanoclusters supported on different materials as catalysts for the selective alkyne semihydrogenation. *Catalysis Today*, 395:34–40, July 2022.
- [42] Ibrahim Karume, Musa M. Musa, Odey Bsharat, Masateru Takahashi, Samir M. Hamdan, and Bassam El Ali. Dual enzymatic dynamic kinetic resolution by thermoanaerobacter ethanolicus secondary alcohol dehydrogenase and candida antarctica lipase b. *RSC Advances*, 6(99):96616–96622, 2016.
- [43] Yan Zhu, Huifeng Qian, Bethany A. Drake, and Rongchao Jin. Atomically precise $\text{Au}_{25}(\text{SR})_{18}$ nanoparticles as catalysts for the selective hydrogenation of α, β -unsaturated ketones and aldehydes. *Angewandte Chemie International Edition*, 49(7):1295–1298, February 2010.

- [44] Runhai Ouyang and De-en Jiang. Understanding selective hydrogenation of α, β – *unsaturated* ketones to unsaturated alcohols on the $\text{Au}_{25}(\text{SR})_{18}$ cluster. *ACS Catalysis*, 5(11):6624–6629, October 2015.
- [45] Vera Truttmann, Christopher Herzig, Ivonne Illes, Andreas Limbeck, Ernst Pittenauer, Michael Stöger-Pollach, Günter Allmaier, Thomas Bürgi, Noelia Barrabés, and Günther Rupprechter. Ligand engineering of immobilized nanoclusters on surfaces: ligand exchange reactions with supported $\text{Au}_{11}(\text{PPh}_3)_7\text{Br}_3$. *Nanoscale*, 12(24):12809–12816, 2020.
- [46] Vera Truttmann, Adea Loxha, Rareş Banu, Ernst Pittenauer, Sami Malola, María Francisca Matus, Yuchen Wang, Elizabeth A. Ploetz, Günther Rupprechter, Thomas Bürgi, Hannu Häkkinen, Christine Aikens, and Noelia Barrabés. Directing intrinsic chirality in gold nanoclusters: Preferential formation of stable enantiopure clusters in high yield and experimentally unveiling the super chirality of Au_{144} . *ACS Nano*, 17(20):20376–20386, October 2023.
- [47] Atal Shivhare, Stephen J. Ambrose, Haixia Zhang, Randy W. Purves, and Robert W. J. Scott. Stable and recyclable Au_{25} clusters for the reduction of 4-nitrophenol. *Chem. Commun.*, 49(3):276–278, 2013.
- [48] Huifeng Qian and Rongchao Jin. Ambient synthesis of $\text{Au}_{144}(\text{SR})_{60}$ nanoclusters in methanol. *Chemistry of Materials*, 23(8):2209–2217, March 2011.
- [49] Scott Calvin. *XAFS for everyone*. CRC Press, Boca Raton, Fla. [u.a.], 2013. Includes bibliographical references and index.
- [50] John J. Rehr, Joshua J. Kas, Fernando D. Vila, Micah P. Prange, and Kevin Jorissen. Parameter-free calculations of x-ray spectra with feff9. *Physical Chemistry Chemical Physics*, 12(21):5503, 2010.
- [51] Matthew Newville. Ifeffit: interactive xafs analysis and feff fitting. *Journal of Synchrotron Radiation*, 8(2):322–324, March 2001.
- [52] Atal Shivhare, Daniel M. Chevrier, Randy W. Purves, and Robert W. J. Scott. Following the thermal activation of $\text{Au}_{25}(\text{SR})_{18}$ clusters for catalysis by x-ray absorption spectroscopy. *The Journal of Physical Chemistry C*, 117(39):20007–20016, September 2013.
- [53] Clara García, Stephan Pollitt, Marte van der Linden, Vera Truttmann, Christoph Rameshan, Raffael Rameshan, Ernst Pittenauer, Günter Allmaier, Peter Kregsamer, Michael Stöger-Pollach, Noelia Barrabés, and Günther Rupprechter. Support effect on the reactivity and stability of $\text{Au}_{25}(\text{SR})_{18}$ and $\text{Au}_{144}(\text{SR})_{60}$ nanoclusters in liquid phase cyclohexane oxidation. *Catalysis Today*, 336:174–185, October 2019.

- [54] Prasenjit Maity, Shinjiro Takano, Seiji Yamazoe, Tomonari Wakabayashi, and Tatsuya Tsukuda. Binding motif of terminal alkynes on gold clusters. *Journal of the American Chemical Society*, 135(25):9450–9457, June 2013.
- [55] Yingli Chen, Xiyun Yang, Linglong Wu, Lirong Tong, and Jing Zhu. Recovery of mg from h₂so₄ leaching solution of serpentine to precipitation of high-purity mg(oh)₂ and 4mgco₃ mg(oh)₂ 4h₂o. *Minerals*, 13(3):318, February 2023.
- [56] Nicole Müller, Rareş Banu, Adea Loxha, Florian Schrenk, Lorenz Lindenthal, Christoph Rameshan, Ernst Pittenauer, Jordi Llorca, Janis Timoshenko, Carlo Marini, and Noelia Barrabés. Dynamic behaviour of platinum and copper dopants in gold nanoclusters supported on ceria catalysts. *Communications Chemistry*, 6(1), December 2023.